CZM Coastal Resilience Grant Program

Feasibility Assessment for Addressing Increased Erosion along the Eel River Inlet Shoreline Due to Barrier Beach Migration

Prepared for:

Town of Falmouth, MA

Prepared by:

Sustainable Coastal Solutions
107A County Road
North Falmouth, Massachusetts 02556

June 2022

TABLE OF CONTENTS

LIST OF FIGURES

LIST OF TABLES

1 INTRODUCTION

The Town of Falmouth received funding assistance through the Massachusetts Office of Coastal Zone Management (MCZM) *FY22 Coastal Resilience Grant Program* to develop an alternatives analysis for mitigating recent erosion of the section of the shoreline along the western side of the Eel River entrance channel. Specifically, Westerly growth of the Washburn Island barrier spit has continued to narrow the tidal channel between the 'hardened' shoreline at the Manauhant Yacht Club, along the western side of the inlet, and the Washburn Island barrier spit to the east. The narrowing of the inlet channel has led to a substantial increase in tidal current velocities that initially led to navigation safety concerns, but now has extended to accelerated erosion along the western shoreline of the inlet, including nearly the complete loss of fringing salt marsh. As the growth and migration of the barrier spit continues to evolve, it is anticipated that increased coastal erosion and constriction of the inlet channel will occur if proactive mitigation efforts are not taken.

Eel River Inlet, located on the south shore of Falmouth, MA, provides a hydraulic connection and tidal exchange between Nantucket Sound and the Eel River estuary (a sub embayment of the larger Waquoit Bay system that is directly linked via the Seapit River; Figure 1.1). The inlet is bounded on the western edge by the armored revetment fronting Menauhant Yacht Club and on the eastern edge by the terminus of the natural barrier beach on Washburn Island. Changes in inlet geometry, experienced by Eel River Inlet, are governed as a response to the growth and migration of the Washburn Island barrier beach.

Barrier beaches are typically long, and narrow landforms separated from the mainland by a body of water or wetland. They are extremely dynamic coastal mechanisms that act as a buffer, protecting low-energy marine environments and the mainland coast by damping wave energy propagating from the open ocean. Barrier beaches evolve both laterally along the coast and transversely shoreward or seaward. Lateral evolution of a barrier spit is governed by longshore sediment transport (also known as littoral drift), growing or receding depending on direction of local transport in relation to the source of sediment. Transversal migration of the barrier beach is caused by cross-shore erosion and/or overwash as a function of incident wave energy and water levels, such that the barrier beach system migrates shoreward in high energy waves with increased water levels and may migrate offshore during low water levels and in low energy wave climates when runup levels are less significant and sediments are deposited near the still water line. Additionally, aeolian transport has the ability to gradually move sediment towards the ocean under dry conditions while winds are blowing offshore, however, the influence of aeolian transport is relatively negligible in comparison to hydrodynamic forcing.

In general, inlets to tidal estuarine systems exist as a result of the balance between the littoral drift and tidal flushing. Wave-induced currents along the open coast transport sediment along the shoreline causing inlet shoaling and/or migration in the direction of the dominant littoral drift. Water elevation differences between the ocean and the estuarine system create tidal flows that prevent inlet closure by providing sufficient water velocity to scour sediments from the main channel. For many natural inlet systems, a period of barrier spit elongation is followed by episodic breaching of the barrier beach, resulting in a more hydraulically efficient inlet channel.

Washburn Island barrier spit is a natural barrier beach peninsula that has maintained a westerly growth trend since its formation more than 80 years ago. Due to the low-lying nature of the natural barrier beach system fronting the Waquoit Bay/Eel River estuarine system, overwash and on-going episodic erosion of the barrier beach spit and subsequent northwestern migration can be anticipated. Additionally, as the spit continues to elongate, the barrier beach becomes narrower and increased hydraulic head between the tide in the ocean and the estuary, due to a lack of efficiency afforded by constricted flow through the inlet, will likely influence a future breach at a narrow "weak" point in the spit (as was previously experienced during Hurricane Bob in 1991).

To address these concerns, information developed from other regional coastal processes analysis efforts, including previous evaluations of water quality and beach erosion studies was utilized to develop an alternatives analysis to evaluate appropriate measures to both mitigate coastal erosion and stabilize the tidal inlet to Eel River. The quantitative analysis of coastal processes builds off of existing data and modeling tools. However, updated bathymetric data, orthoimagery, and expanded numerical modeling methods that incorporate tidal hydrodynamics, waves, and sediment transport were required to provide appropriate analysis tools for evaluating management options. The overall goal of the planning analysis was to improve long-term resiliency along the shoreline immediately west of Eel River Inlet as well as increase navigational safety within the inlet channel.

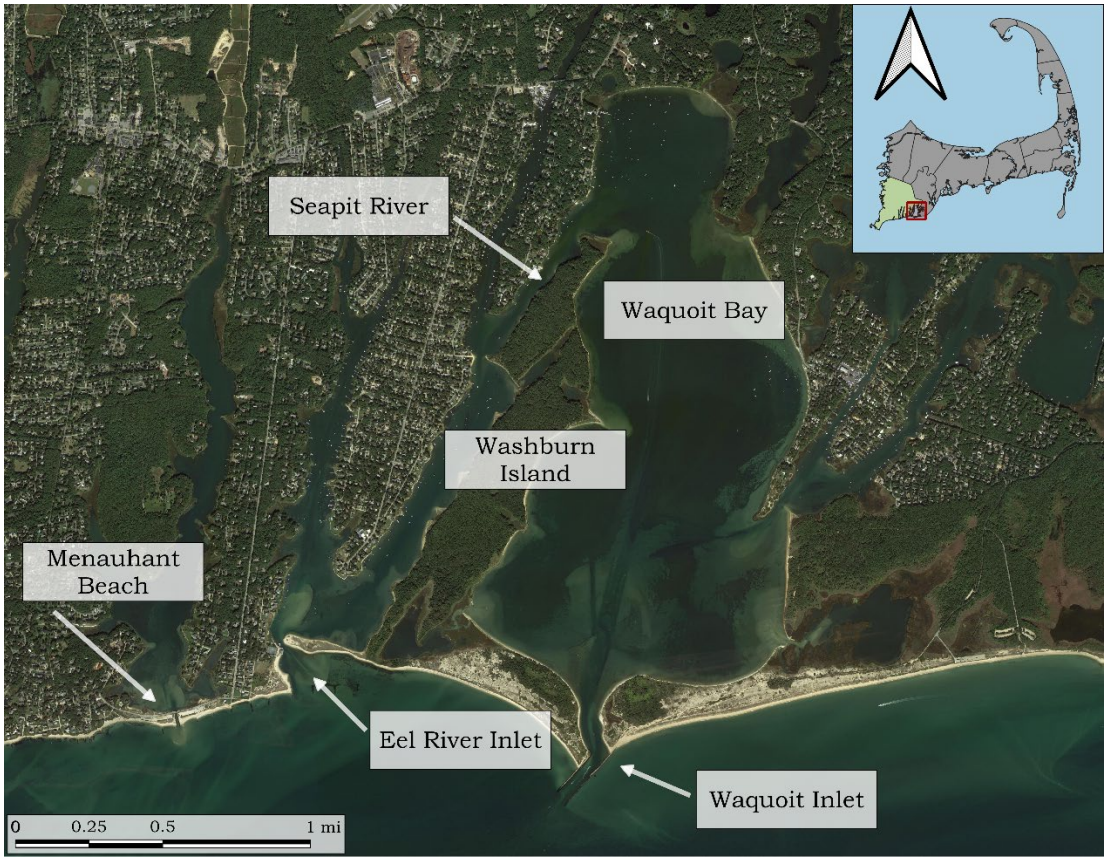

Figure 1.1 Aerial image of the Waquoit Bay system (credit: Google, 2016)

2 EVOLUTION OF THE COAST AND ENVIRONMENTAL CONDITIONS

The Eel River Inlet is located on the south shore of Falmouth, MA, between the eastern edge of Menauhant Beach and the distal end of the barrier beach on Washburn Island (Figure 1.1). The inlet allows tidal exchange between Nantucket Sound and the Eel River estuary (a sub embayment of the larger Waquoit Bay system). The Eel River estuary is directly linked to Waquoit Bay through the Seapit River, allowing for additional tidal flushing of the upper reaches of the system.

2.1 Site History

The south-facing coast of the Upper Cape was formed from marine deposits in an outwash plain as the Laurentide ice sheet receded after the Wisconsinan glacial stage. Due to the low-lying nature of glacial out wash plains, the south-facing coast of Cape Cod is comprised of many estuaries and lagoons that have been formed by flooded erosion furrows, kettle holes and ground water sapping. Naturally these bodies of water are protected by baymouth beaches and barrier islands. The littoral sediments between Falmouth Heights and the Waquoit Bay inlet are generally medium and fine grain sands eroded from glacial till and sandy deposits from littoral currents. Conversely, the shoreline sediments from Nobska Point eastward to Falmouth Harbor are morainal due to the proximity of the Buzzards Bay Moraine and generally consist of mixed cobbles and more coarse sands.

Originally, the Waquoit Bay system consisted of a single inlet at the southern end of Waquoit Bay and tidal exchange in the western bay (Eel River) was governed solely by flows passing through the Seapit River due to a thin barrier beach spanning from Menauhant Beach to Washburn Island separating it from Nantucket Sound (Figure 2.1a). However, extreme tides and storm waves during the storm of 1938 washed over the barrier beach and created an inlet directly south of the Menauhant Yacht Club. The newly formed breach remained open naturally until it was filled with material and closed off by the United States Army Corps of Engineers (USACE) in 1941 to provide access to Washburn Island, which was utilized as a military training facility at the time (Figure 2.2). The barrier beach was stabilized by the implementation of several shore-perpendicular groins and jetties. Following the end of the war, the barrier beach was dredged to reopen the inlet to Eel River (Figure 2.1b). Following the reopening of Eel River Inlet, a deficit in sediment supply caused by groins and jetties to the west as well as the northerly migration of the Washburn Island spit has resulted in the eastern groins becoming ‘flanked’, or separated from the beach. Once detached, the groins are unable to provide proper function stabilizing the shoreline causing the rate of retreat of the spit to increase as shown in Figure 2.1c.

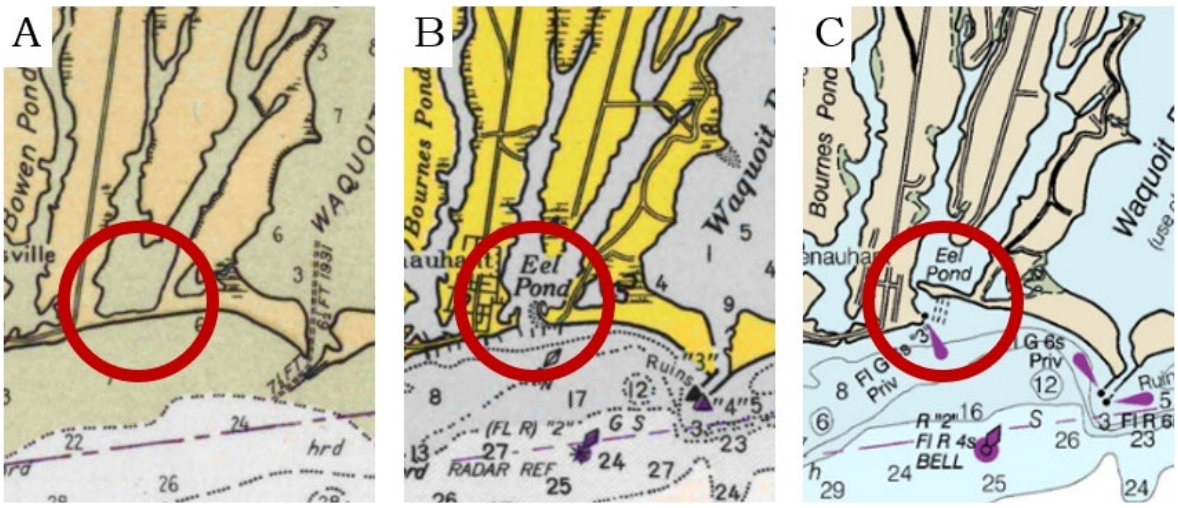

Figure 2.1 Historical Nantucket Sound and Approaches nautical charts (chart number: 1209) from the National Oceanic and Atmospheric Administration (NOAA), formerly the United States Coast and Geodetic Survey (USC&GS), showing the shoreline change between the years (a) 1933, (b) 1966, and (c) 2019.

Figure 2.2 Beach landing training on Washburn Island (credit: CapeNews.net)

2.2 Shoreline Change

The southern coast of Cape Cod is a dynamic coastal region, where natural wave and tidal forces continue to reshape the shoreline. Due to the protection afforded by the islands of Marthas Vineyard and Nantucket, the south shore of Cape Cod is protected from the influence of long period open ocean wave conditions. Similar to many portions of the Massachusetts coast, the available sediment supply influences the migration and/or stability of tidal inlets and their associated barrier beach systems. Tidal inlets can become overwhelmed by the gradual wave-driven migration of a barrier beach separating the estuaries from the ocean. In addition to these natural coastal processes, man-made structures often can influence the stability of a barrier/inlet system.

Typical of many shorelines in the region, the shorelines of Menauhant and Washburn Island were strongly influenced by anthropogenic development to improve navigation and protect upland infrastructure (Figure 2.3). Shoreline stabilization structures provide protection from erosion to upland areas but by doing so, they trap littoral sediments creating a deficit in longshore transport to down drift beaches. The discontinuity in littoral drift increases the rate of erosion on unprotected beaches down-stream. The dramatic retreat of the Washburn Island spit due to the lack of sediment supply and abandoned stabilization structures can be seen in the over the 150-year shoreline position record, shown in Figure 2.4. Originally anchored with a series of three shore-perpendicular stone groins, Washburn Island spit has retreated landward (to the north) over 1000 feet near the distal end of the spit subsequent to the groins becoming flanked and were no longer able to provide structural function in maintaining the position of the barrier beach. The eastern end of the barrier spit remains attached to Washburn Island, held in place by the natural protection of mixed cobble glacial deposits that make up the geologic composition of the island (Figure 2.5). Increased stabilization provided by the cobble along this region of the beach has caused the landward retreat of the shoreline to be much less dramatic than the distal end of the spit; thereby creating a gradient in shoreline change between the island and the western end of the spit that has caused the barrier beach to have a quasi-rotational growth to the northwest (Figure 2.6).

Figure 2.3 Public and Private shoreline stabilization structures, inventoried in 2009 and 2013, respectively. (Inventory Source: Mass GIS).

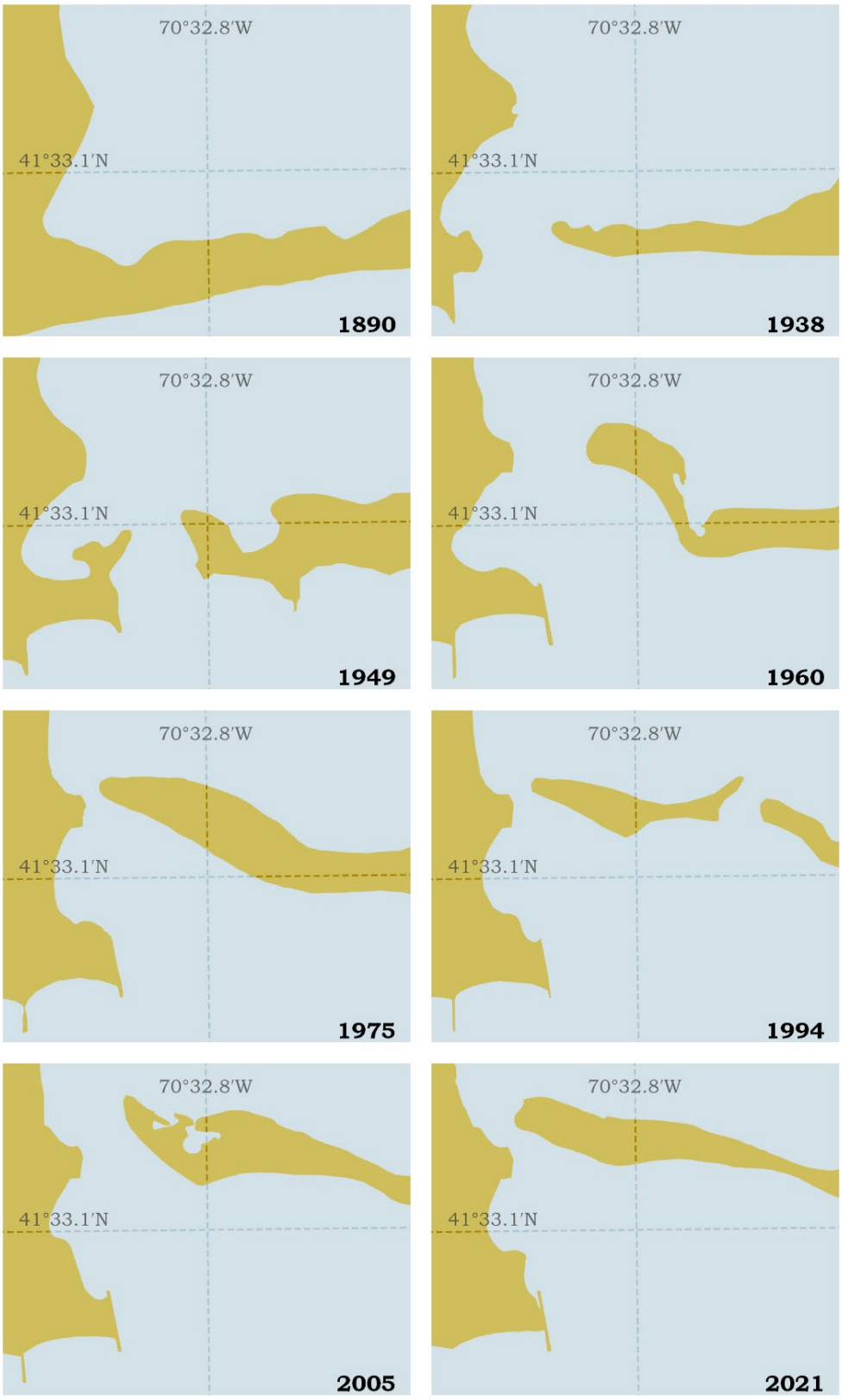

Figure 2.4 Morphological change of Eel River Inlet and Washburn Island spit from 1890 to 2021.

Figure 2.5 Mixed cobble sediments anchoring the barrier spit to Washburn Island.

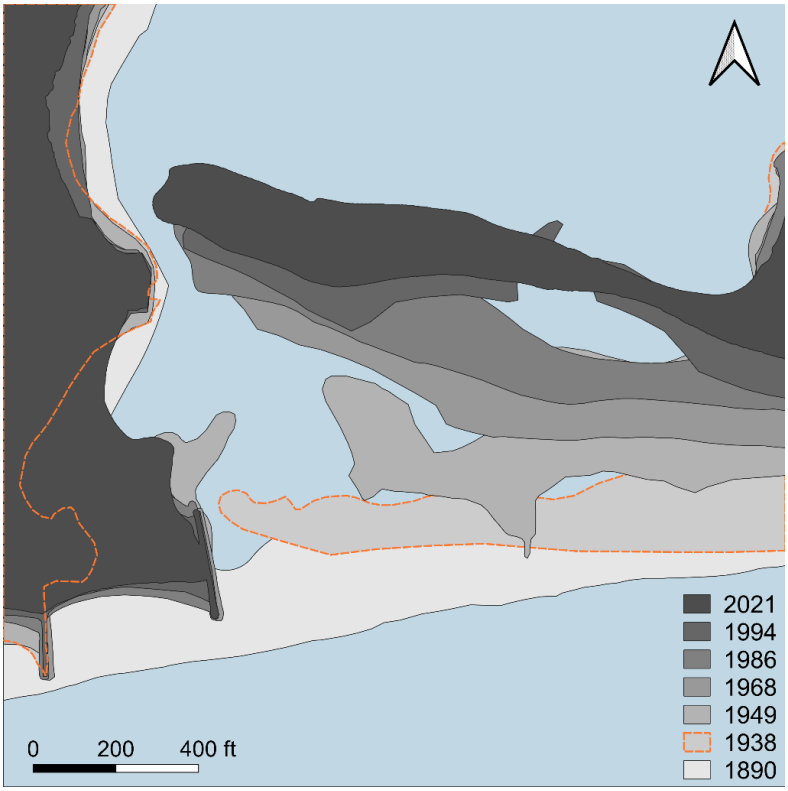

Figure 2.6 Comparison of the evolution of the distal end of the barrier spit relative to the main shoreline of Washburn Island from 1890 to 2021.

Eel River Inlet is bounded by an armored stone revetment on the western edge and the terminus of the barrier spit on the eastern edge. The stone revetment fronting the Menauhant Yacht Club on the western shoreline of the inlet has contributed to anchoring the inlet location in place as well as helping it remain relatively stable. Although constricted, the inlet allows for effective tidal circulation due to the stability of the inlet opening maintained during ebb flows by the back pressure of the embayment system. However, north-westerly elongation of the barrier spit has altered the direction of tidal flows and increased flow velocity due to inlet constriction, effectively creating increased hydraulic stress on the shoreline north of the Menauhant Yacht Club. The redirected influence of the tidal flow has caused an increased rate of erosion as well as scarping and slumping of the existing fringe marsh along the shoreline (Figure 2.7). Notably, this increased rate of erosion was observed over the past 10-15 years. Before then this section of shoreline has remained relatively stable (Figure 2.8). Specifically, Figure 2.8 illustrates the rather negligible change along the shoreline north of Menauhant Yacht Club during the 41-year span between 1968 and 2009, compared to the much more appreciable change observed during the 12-year span between 2009 and 2021.

Use of shoreline change information allows quantification of coastal processes by providing a measure of nearshore accretion or erosion. In general, accurate shoreline data sets cover a significantly longer period of time than bathymetric data sets. While the U.S. Coast & Geodetic Survey historically collected detailed bathymetry information, the spatial coverage is sparse relative to contemporary surveying methods and data sets. Therefore, these older data can produce inaccurate results when utilized for small-scale coastal change assessments. For the shoreline in the vicinity of Eel River Inlet, high quality shoreline data sets are available dating back to the mid-1800s. This 150+ year time period covers the evolution of shoreline response from unaltered natural beach/dune system to the armored shoreline that exists today.

Rates of change in high-water shoreline position for the time interval between October 2009 and September 2021 were evaluated from the eastern end of Menauhant beach to the northern extent of the unprotected shoreline north of Menauhant Yacht Club, as well as the shoreline encompassing the Washburn Island barrier spit (Figure 2.9). The 2009 shoreline position was delineated using aerial orthoimagery and corroborated with supplemental topographic LiDAR datasets. The constructed shoreline was then visually compared to a shoreline of the same year produced by the U.S. Geological Survey (USGS) in cooperation with the Massachusetts Office of Coastal Zone Management (MA CZM) for quality assurance. The 2021 shoreline was measured using a Leica Viva C515 RTK GPS. The location of the survey points collected by the GPS was determined visually from morphologic features present on the beach and/or from a debris line when available.

Cross-shore transects used to calculate the rate of change were made at 25-foot intervals using SMS Aquaveo. The shore-normal transects were developed using average shoreline angles determined at each analysis point. All transects used for determining change rates were visually inspected to ensure suitability for analysis and shoreline structure avoidance. The data output is a table of shoreline change magnitudes and rates for each transect where shoreline change denoted with a minus sign represents erosion.

The computed change rate transects, shown in Figure 2.9, show that the maximum erosional rates were experienced along the shoreline north of Menauhant Yacht Club and the south-facing shoreline of the Washburn Island Spit with rates of 6.5 and 6.6 feet per year, respectively. The large rates of erosion observed on the spit are likely due to the

‘bulb’ of sand dissipating westward illustrated by the adjacent area of accretional transects. The general evolution of the spit shows a narrowing and westward elongation trend towards the distal end. This migration of sediment may indicate a strong westward flow during flood tide cycles due to the orientation of the inlet. This postulation is further exhibited by the area of maximum erosion on the western shoreline, where it is exposed to flood tide currents which have increased overtime due to channel constriction.

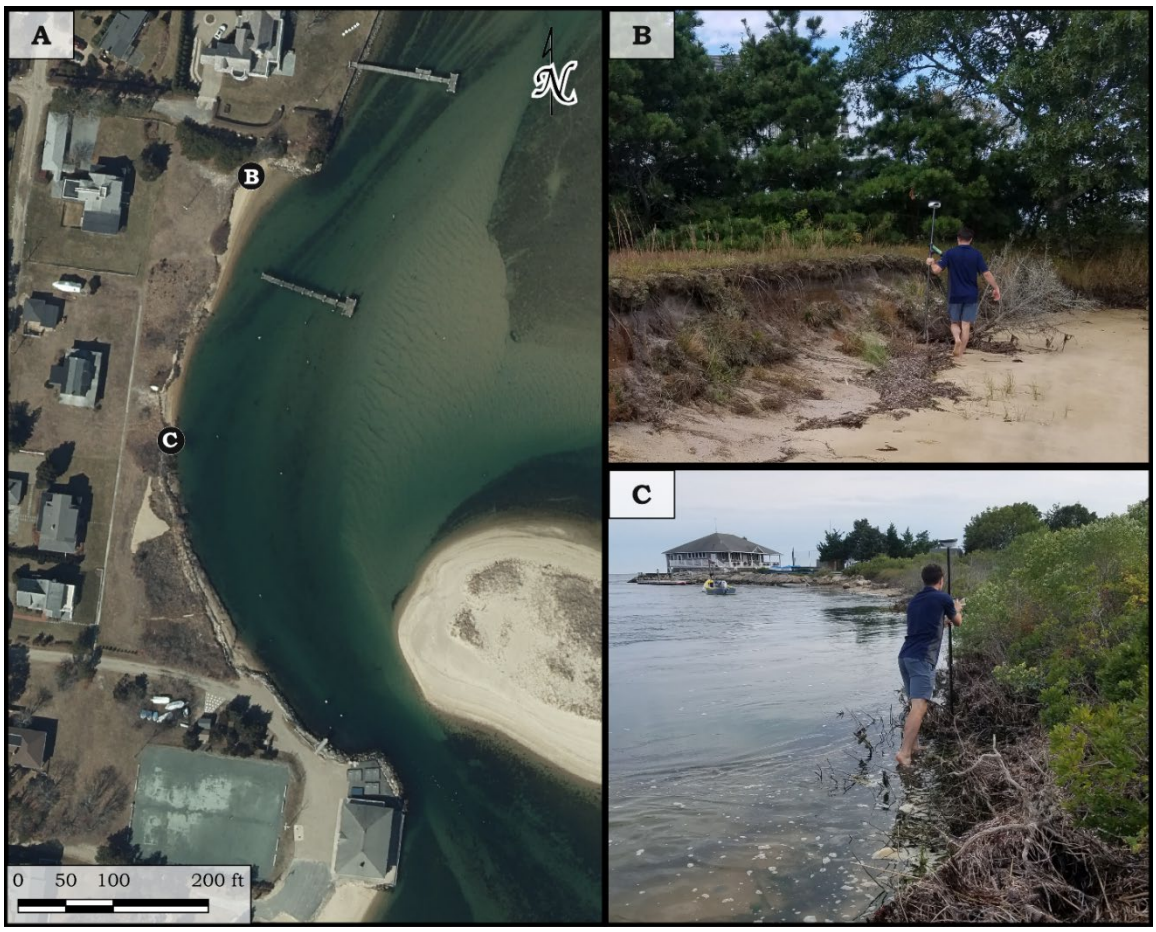

Figure 2.7 (A) 2021 aerial image of the shoreline immediately north of Menauhant Yacht Club. (B) Erosional scarp on the northern region of the shoreline, photo oriented to the north. (C) Complete loss of the beach and continual degradation of fringing marsh and wetland vegetation, photo oriented to the south.

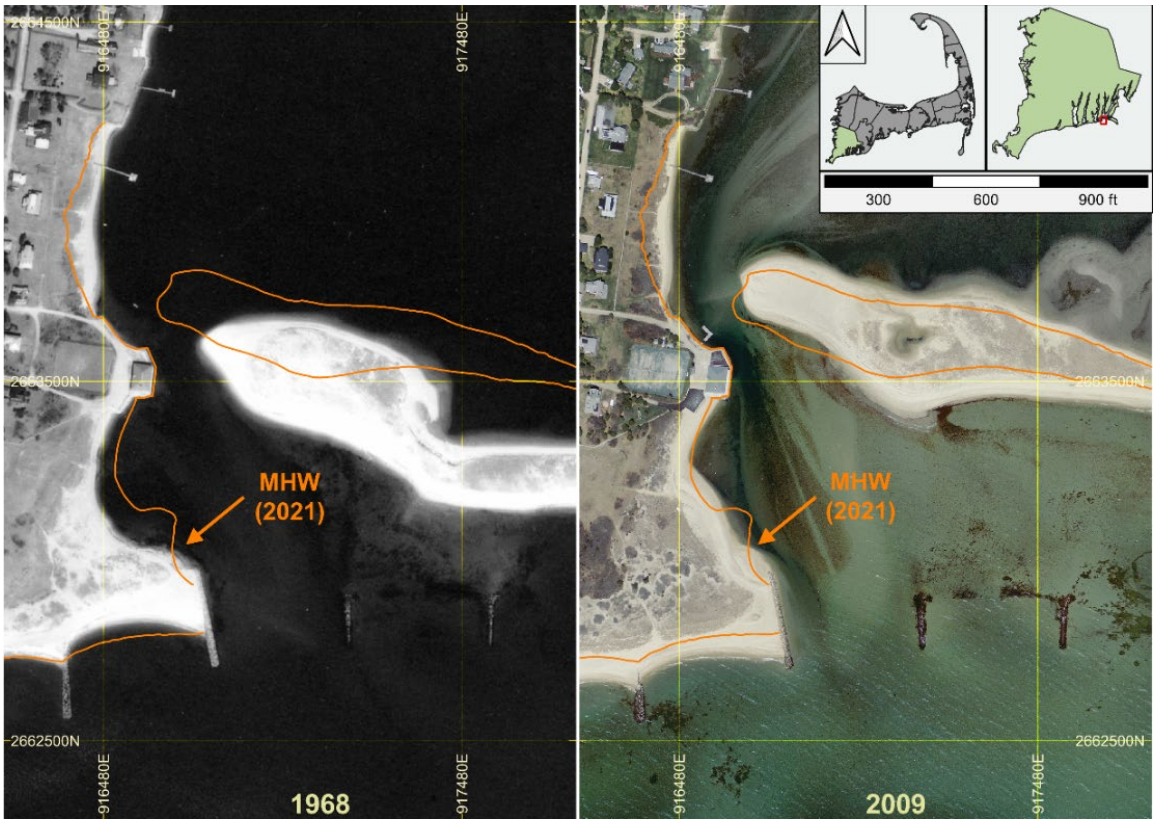

Figure 2.8 Aerial Imagery comparison of Eel River Inlet in 1968 (left) and 2009 (right). The orange line denotes the MHW shoreline surveyed in September 2021.

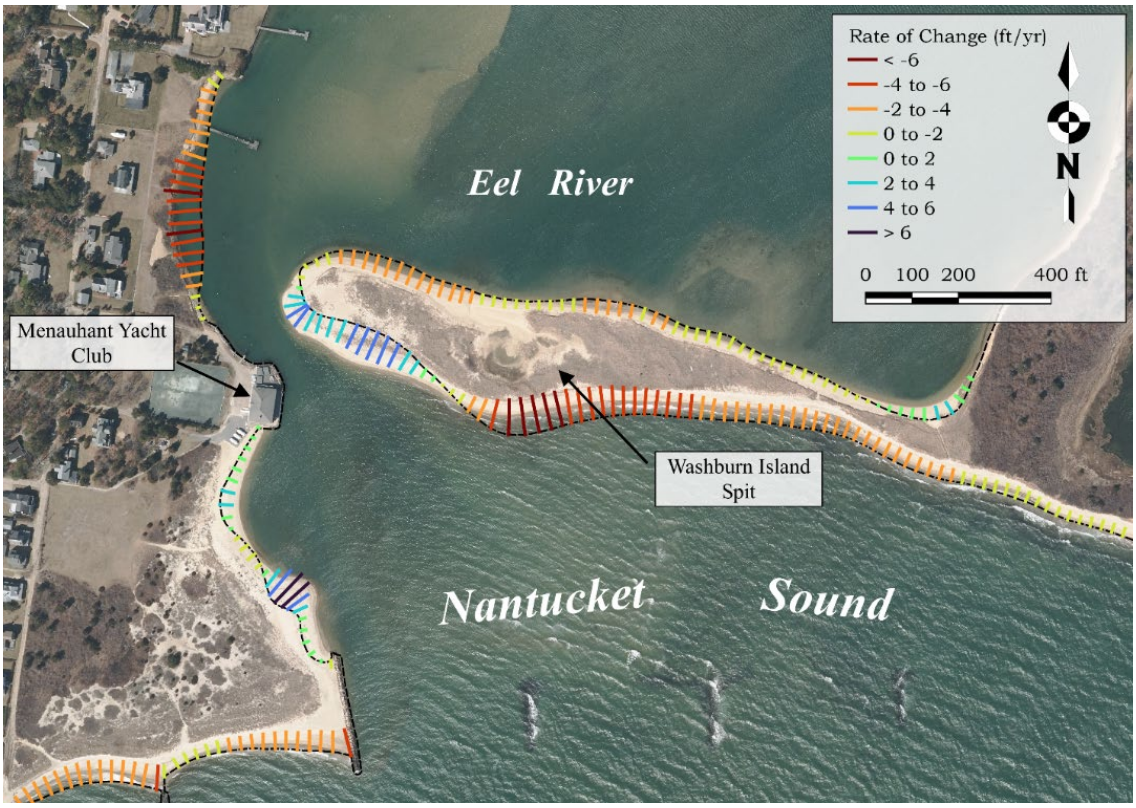

Figure 2.9 Shoreline change transects for Washburn Island barrier beach and the western shoreline adjacent to Eel River Inlet, between October 2009 and September 2021, plotted on USGS Color Ortho Imagery (3/24/2019 to 4/25/2019). Transect lengths indicate the linear change magnitude between shorelines, while the color scale represents the average annualized rate of change, as indicated by the legend. The 2009 shoreline is denoted by the black dashed line.

2.3 Bathymetric Change

Bathymetric and topographic data collected from Light Detection and Ranging (LiDAR) were used to provide three dimensional surfaces of topographic, as well as limited nearshore bathymetric, information that could be evaluated within appropriate mapping software. Ideally, multiple LiDAR datasets could be examined sequentially to look at bathymetric change over areas of overlapping survey coverage. However due to a lack of abundant LiDAR data in the area, a comparison between only two survey years could be made. Specifically used were data from the New England District of the USACE made available from surveys flown in spring, 2010 and 2018. These data were used to calculate evolutionary changes of physical features identified in aerial imagery (Figure 2.10). The changes, shown in Figure 2.11, denote significant erosion and bottom scouring along the western shoreline north of Menauhant Yacht Club, as well as sediment deposition resulting in farther expansion of the barrier spit into the inlet. Accretion of the flood and ebb shoals denotes the relative changes in inlet location and hydrodynamics over the eight-year span between bathymetric datasets. Other features that indicate the historical evolution of the barrier system, such as the overwash fan and secondary inlet scar, have remained relatively in place indicating the short term (~ 10 years) stability of the spit.

Figure 2.10 Map of Eel River Inlet and Washburn Island spit, as well as specific physical features created by the historical evolution of the barrier system.

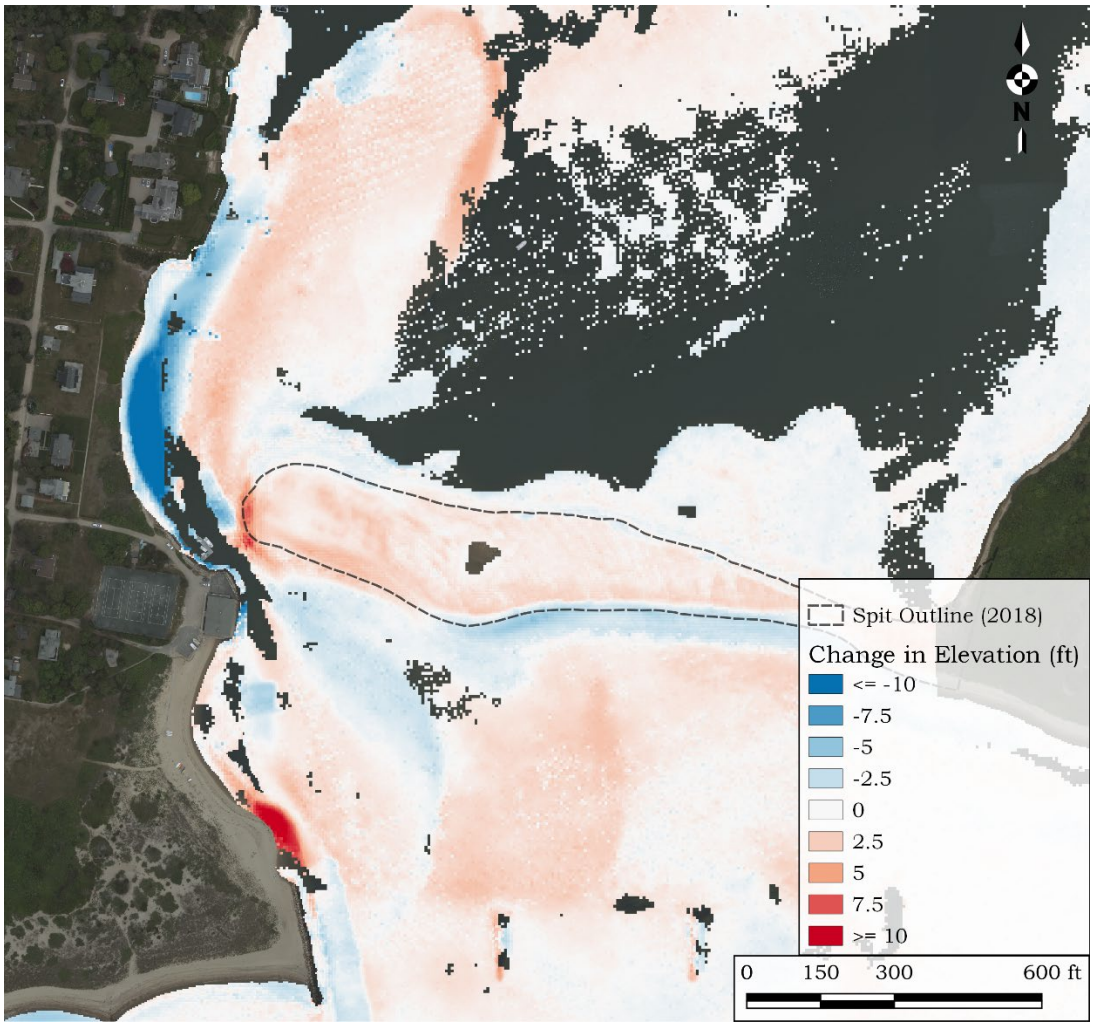

Figure 2.11 Bathymetric change from 2010 to 2018 for the nearshore area in the vicinity of Eel River Inlet. Topographic change for the Washburn Island spit is included also, outlined by the black dashed line. Colors indicate amount of change, where blues denote erosion and reds denote accretion.

3 COASTAL PROCESSES

A fundamental understanding of the existing environment and coastal processes surrounding the Eel River estuary is critical to evaluating potential management strategies. Assessment of current bathymetric and hydrodynamic conditions will control the feasibility of the proposed alternatives as well as aid in the estimation of hydrodynamic and morphological response to any alterations made to the inlet channel or adjacent shorelines.

3.1 Tide Analysis

Tide data records used in this study were measured at six stations in the Waquoit Bay system: 1) offshore Eel River Inlet, 2) Eel River West, 3) Childs River, 4) Waquoit Bay, 5) Hamblin Pond, and 6) Great River. The locations of the tide collection stations are shown in Figure 3.1. The gauges used to record the tide data were deployed between January 18, 2002 and February 19, 2002. All gauges were deployed longer than the 29-day minimum required to record the monthly maximum and minimum astronomical tide ranges, and also to provide a record of sufficient length to perform a harmonic analysis to determine the 23 main tidal constituents at the gauge locations. The elevation of each gauge was surveyed relative to NGVD29 and converted to NAVD88 using NOAA's VDATUM. Data from the offshore record were used to develop the open boundary condition of the hydrodynamic model. Data from the other five locations were used to calibrate the model.

The tides in the Waquoit Bay system are semi-diurnal, meaning that there are typically two complete tide cycles in a day. Plots of tide data from the six gauges are shown in Figure 3.2, for approximately two 12.4-hour tide cycles, near the spring tide maximum (full moon occurred January 28, 2002). This plot demonstrates the slight variation in the time and elevation of the high and low tides across the measurement stations. These tidal phase (delay) differences provide potential for flow through the Waquoit Bay system, in addition to the potential supplied by the rise and fall of the tide offshore.

Figure 3.1 Tide gauge locations used in the MEP water quality report for the Waquoit Bay and Eel River embayment systems.

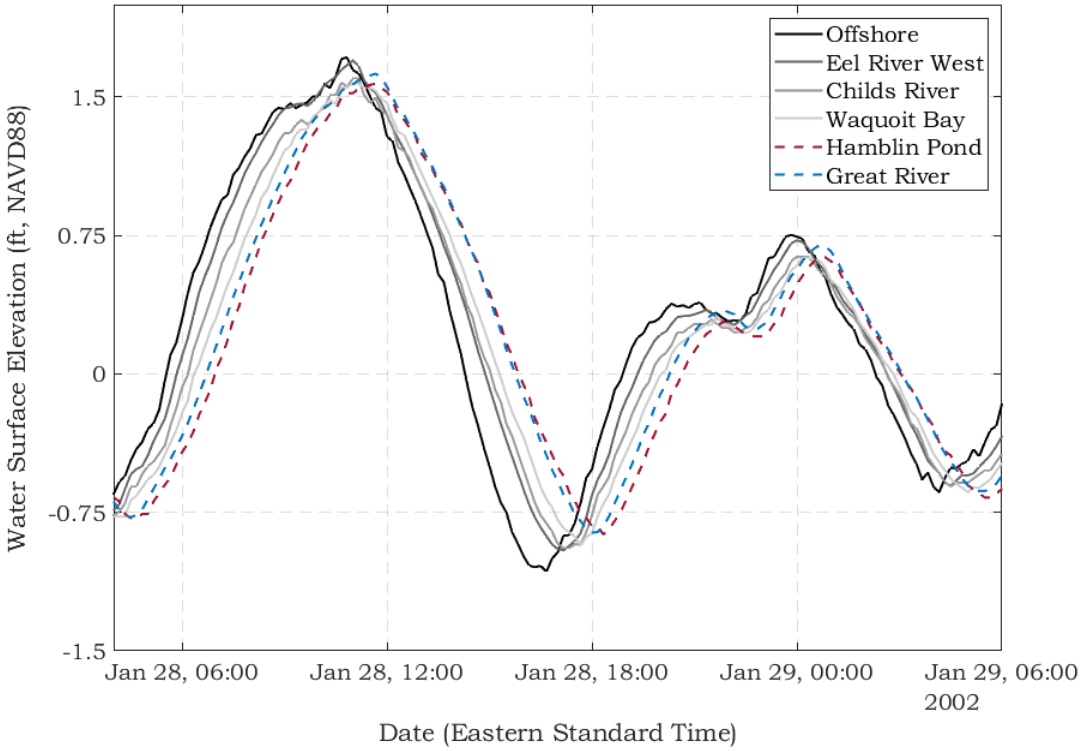

Figure 3.2 Plot showing two tide cycles at the six tide gauge locations in Waquoit Bay system plotted together. Demonstrated in this plot is the tidal phase and amplitude differences across the system. The time lag of low tide from the offshore gauge and the gauge located in Hamblin Pond, from this plot, is approximately 1 hour and 40 minutes.

Standard tide datums were computed from the tide records. These datums are presented in Table 3.1. For most NOAA tide stations, these datums are computed using 19 years of tide data, the definition of a tidal epoch. For this study, a significantly shorter time span of data was available, however, these datums still provide a useful comparison of tidal dynamics within the system. The Mean Higher High Water (MHHW) and the Mean Lower Low Water (MLLW) levels represent the mean of the daily highest and lowest water levels, respectively. The Mean High Water (MHW) and Mean Low Water (MLW) levels represent the mean of all high and low tides of a record. The mean Tide Level (MTL) is simply the mean of MHW and MLW. The MTL, MLW, and MLLW levels at the Hamblin Pond and Waquoit Bay stations show that maximum attenuation of the tide occurs in the inner regions of the embayment system where tidal exchange is typically less efficient.

In addition to computing the standard tide datums, a more thorough harmonic analysis of the six tidal data sets was performed to produce the tidal amplitude and phase of the major tidal constituents. This analysis also yielded quantitative assessment of the relative influence of non-tidal, or residual, processes (such as wind forcing) on the hydrodynamics of the system. Harmonic analysis is a mathematical procedure that fits sinusoidal functions of the known frequency to the measured signal. The observed astronomical tide is therefore the sum of several individual tidal constituents, with a

particular amplitude and frequency. For demonstration purposes a graphical example of tidal constituents add together is shown in Figure 3.3, where the observed tide is equal to the superposition of the various constituent curves shown. The amplitudes and phase of the 23 known tidal constituents result from this procedure. Table 3.2 presents the amplitudes of eight constituents at the six tide gauge stations in the Waquoit Bay system.

Table 3.1 Tide datums computed from data records collected offshore of the Eel River inlet entrance channel and in the upper regions of Eel River West, Child's River, Waquoit Bay, Hamblin Pond, and Great River (January 18, 2002 to February 19, 2002). Datum elevations are given relative to NAVD88.

Tide Datum	Offshore	Eel River West	Child's River	Waquoit Bay	Hamblin Pond	Great River
Maximum Tide	1.86	1.86	1.73	1.70	1.71	1.74
MHHW	1.15	1.14	1.10	1.07	1.06	1.09
MHW	0.79	0.76	0.74	0.72	0.71	0.74
MTL	-0.07	-0.06	-0.06	-0.05	-0.04	-0.06
MLW	-0.92	-0.88	-0.86	-0.83	-0.79	-0.86
MLLW	-1.15	-1.06	-1.06	-0.98	-0.92	-1.02
Minimum Tide	-1.88	-1.52	-1.78	-1.35	-1.45	-1.56

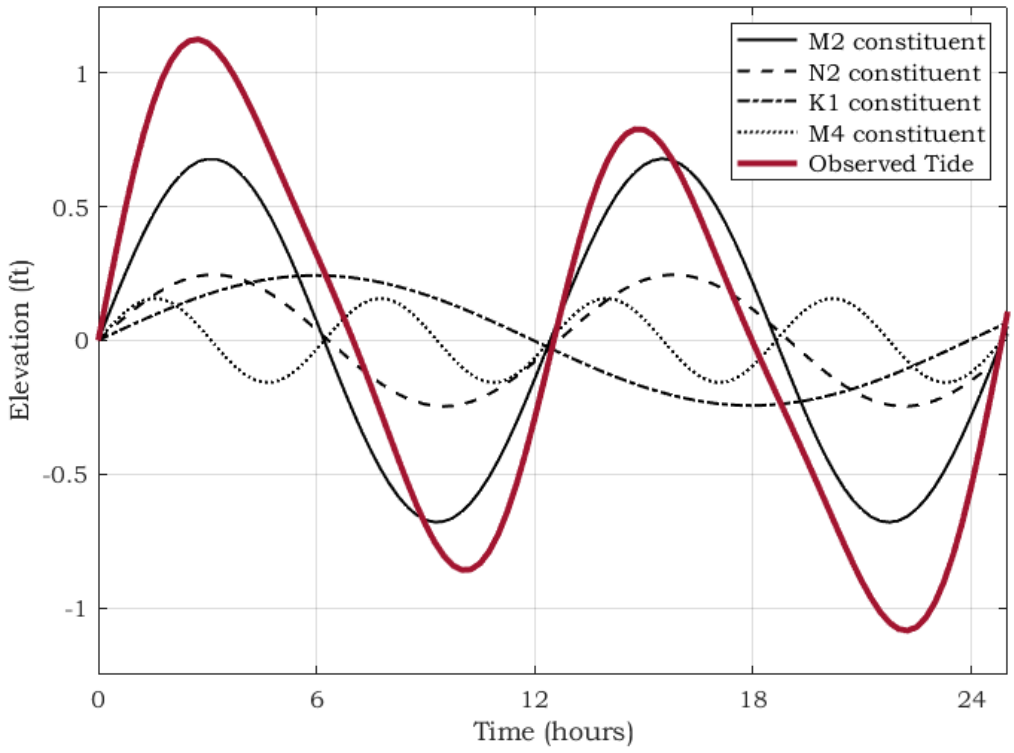

Figure 3.3 Example of an observed astronomical tide as the sum of its primary constituents.

Table 3.2 Major tidal constituents determined for gauge locations in the Waquoit Bay system (January 18, 2002 to February 19, 2002)								
	Amplitude (feet)							
Constituent	M_2	M_4	M_6	S_2	N_2	K_1	O_1	M_{sf}
Period (hours)	12.42	6.21	4.14	12.00	12.66	23.93	25.82	354.61
Offshore	0.68	0.16	0.05	0.07	0.25	0.24	0.24	0.03
Eel River West	0.66	0.13	0.06	0.06	0.23	0.26	0.24	0.02
Child's River	0.64	0.11	0.05	0.06	0.22	0.24	0.24	0.02
Waquoit Bay	0.64	0.09	0.04	0.06	0.22	0.24	0.24	0.02
Hamblin Pond	0.63	0.07	0.05	0.06	0.21	0.24	0.24	0.03
Great River	0.65	0.09	0.05	0.06	0.22	0.24	0.24	0.04

The M_2, or the familiar twice-a-day lunar semi-diurnal tide, is the strongest contributor to the signal with an offshore amplitude of 0.68 ft. The total range of the M_2 tide is twice the amplitude, or 1.36 ft. The M_4 and M_6 tides are higher frequency harmonics of the M_2 lunar tide (exactly half the period of the M_2 for the M_4, and one third of the M_2 period for the M_6), and result from frictional attenuation of the M_2 tide in shallow water. The other major tide constituents show little variation across the system. The S_2 is the largest solar constituent and is related to the gravitational forces of the Sun on the tides. Like the M_2, the S_2 (12.00-hour period) is a semi-diurnal tidal constituent; however, because the sun is much farther from the Earth the amplitude of the S_2 is usually much smaller than the M_2. The effects of the S_2 are most commonly seen in spring tides and neap tides, during which the Sun and Moon are either aligned or perpendicular, respectively, creating a beat phenomenon. The amplitude of the S_2 provides a relatively small contribution (0.06 feet) to the tidal fluctuation and is consistent across all of the regions in the Waquoit Bay system. The M_{sf} is a lunarsolar fortnightly constituent with a period of approximately 14 days, and is the result of shallow water interactions occurring from the periodic conjunction of the sun and moon. The M_{sf} has an offshore amplitude of 0.03 feet. The other semi-diurnal tide, the N_2 (12.66-hour period) tide, contributes across the system to varying degrees offshore amplitudes of 0.25 feet. The variation of the N_2 is often related to the variation observed by the M_2 constituent because the N_2 is a result of the 27-day variation in the Moon's distance to the Earth. The diurnal tides (once daily), K_1 and O_1, both possess amplitudes of approximately 0.25 feet.

Along with the variation in constituent amplitudes throughout the system, the phase change of the tide is seen from the results of the harmonic analysis. Table 3.3 shows the delay of the M_2 at different points in the Waquoit Bay system, relative to the timing of the M_2 constituent offshore of the Eel River inlet entrance channel. The greatest delay is at the Hamblin Pond gauge station, which also showed the largest reduction of the M_2 amplitude (Table 3.2). Compared to other locations instrumented in this study, the Hamblin Pond station shows the greatest tidal attenuation compared to the tide offshore.

Table 3.3	M_2 tidal constituent phase delay (relative to tides immediately offshore Eel River Inlet) for gauge locations in the Waquoit Bay system, determined from measured tide data.
Station	Delay (minutes)
Eel River West	23.4
Child's River	33.6
Waquoit Bay	46.7
Hamblin Pond	72.8
Great River	64.6

In addition to the harmonic analysis, the tide data were further evaluated to determine the importance of tidal versus non-tidal processes to changes in water surface elevation. These other processes include wind forcing (set-up or set-down) within the estuary, as well as sub-tidal oscillations of the sea surface (e.g., caused by large scale weather systems). Variations in water surface elevation can also be affected by freshwater discharge into the system, if these volumes are relatively large compared to tidal flow.

The results of the analysis to determine the energy distribution (or variance) of the original water elevation time series for the Waquoit Bay system is presented in Table 3.4, and is compared to the energy content of the astronomical tidal signal (recreated by summing the contributions from the 23 constituents determined from the harmonic analysis). Subtracting the tidal signal from the original elevation time series (measured data) resulted with the non-tidal, or residual, portion of the water elevation changes. The energy of this non-tidal signal is compared to the tidal signal, and yields a quantitative measure of how important these non-tidal physical processes can be to hydrodynamic circulation within the estuary. Figure 3.4 shows the comparison of the measured tide from outside Eel River Inlet, with the computed astronomical tide resulting from the harmonic analysis, and the subsequent non-tidal residual. Atmospheric contributions on the tides that may seem small in other areas of New England can influence rather large impacts in the Waquoit Bay system due to the relatively small tidal range in the vicinity of Eel River Inlet. The tidal residual is seen to be generally less than 1 foot throughout the deployment period; however, in many instances the magnitude of the residual tide is larger than the predicted tide.

Table 3.4 shows that there is a reduction in tidal energy in areas farther from the inlet. This is another indication of the tidal attenuation through the system. The analysis also shows that tidal processes are responsible for approximately 64% of the water level changes in the Waquoit Bay system. The remaining 36% was the result of atmospheric forcing, due to winds or barometric pressure gradients. The small contribution of the residual to the complete tide signal provides confidence that the system can be adequately modeled using tide data series.

Table 3.4 Percentages of Tidal versus Non-Tidal Energy for the Waquoit Bay system, January 18 to February 19, 2002			
Tide Gauge Location	Total Variance ($ft^2 \cdot sec$)	Tidal (%)	Non-tidal (%)
Offshore Eel River Inlet	0.502	64.5	35.5
Eel River West	0.484	63.5	36.5
Child's River	0.450	63.4	36.6
Waquoit Bay	0.438	63.5	36.5
Hamblin Pond	0.416	64.2	35.8
Great River	0.452	63.5	36.5

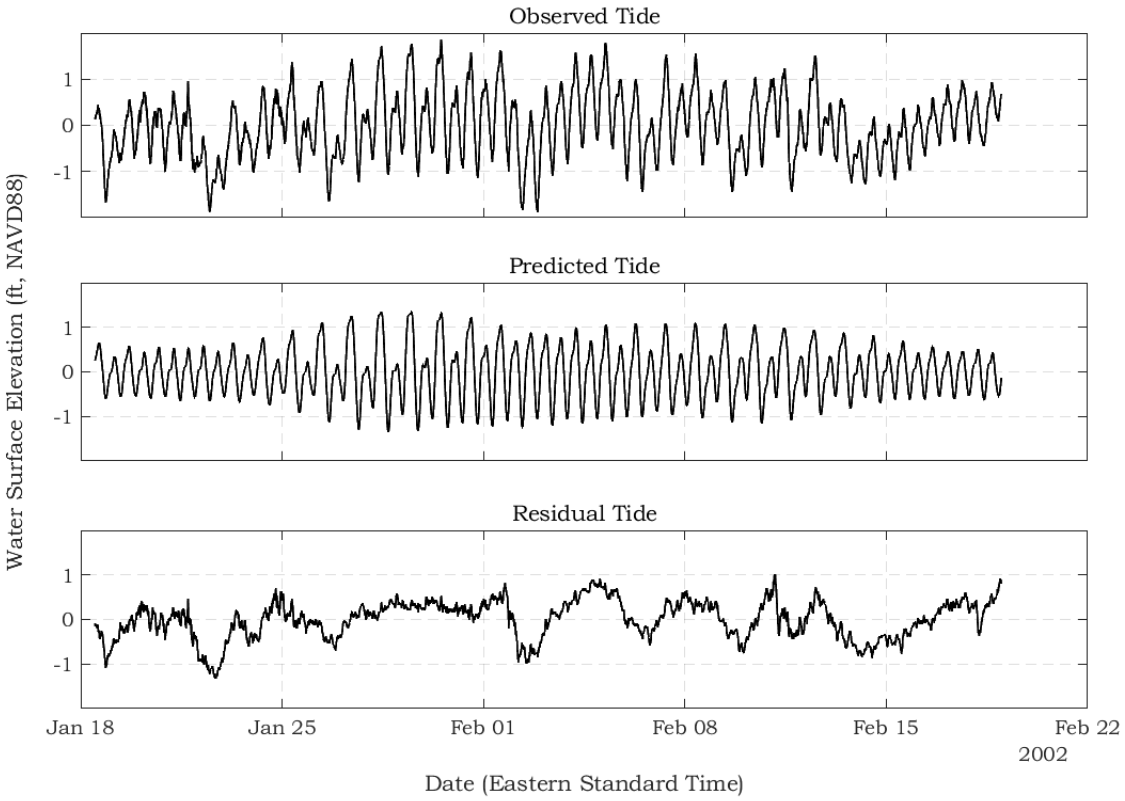

Figure 3.4 Plot showing the comparison between the measured tide time series (top plot), and the predicted astronomical tide (middle plot) computed using the 23 individual tide constituents determined in the harmonic analysis of the Waquoit Bay system gauge data. The residual tide shown in the bottom plot is computed as the difference between the measured and predicted time series.

3.2 Offshore Wind and Wave Data

Wave and wind conditions were generated using the data available from the USACE WIS hindcast database from station 63082 and the Buzzards Bay C-MAN Station (BUZM3), respectively (Figure 3.5). The WIS station is located approximately 13 miles southwest of Nantucket and has a record that spans the 38-year period between January 1980 and December 2019 (Figure 3.6). Each hourly WIS time step includes parameters that describe the wave characteristics (e.g., swell direction θ; significant wave height, H_s; and corresponding mean wave period, T_m). The C-MAN station is a meteorological platform operated by NOAA's National Data Buoy Center (NDBC) located approximately 4 miles west-southwest of Cuttyhunk Island and has an hourly wind record spanning 35 years from August 1985 to present as well as continuously wind data records spanning from May 1997 to present (Figure 3.7).

For the wave data of the WIS hindcast, south is the predominant sector. Waves propagate from this direction 19.3% of the time. 86.8% of waves from this sector have a height less than 6 feet. Due to the protection afforded by Marthas Vineyard, Eel River is most vulnerable to waves propagating from the southeast to east sectors. Waves from these sectors contribute to a combined 28.6% of the wave record with more than half of that coming from the southeast alone. It should be noted that the WIS station represents measurements south of the Muskeget Channel that are generally more protected from waves propagating from the ENE to WNW sectors by the islands of Nantucket, Marthas Vineyard, and Cape Cod, likewise the vicinity of Eel River Inlet is also protected against wave forces from these directions. Additionally, waves from the WSW to the SSW sectors typically consist of higher percentages of waves larger than 6 feet, however, the Falmouth shoreline and entrance Eel River Inlet are is generally sheltered from wave events from these directions. Furthermore, nearshore wave heights often vary from those measured offshore, in deep water, due to shallow water bathymetry and bottom effects changing the physical shape of the waves.

Figure 3.5 Map showing the locations of NDBC station BUZM3 and WIS hindcast station 63082.

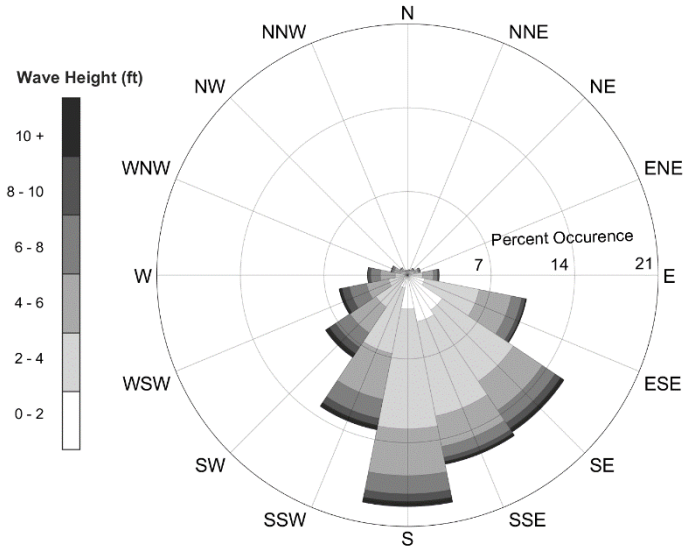

Figure 3.6 Hourly wave data collected from the WIS hindcast station 63082 (southwest of Nantucket) for the 40-year period between January 1980 and December 2019. Direction indicates from where the waves were propagating. Wind speeds are color coordinated such that larger magnitudes correspond to darker gray tones. Combined length of segments in each sector indicates percent occurrence of all wave heights from that direction.

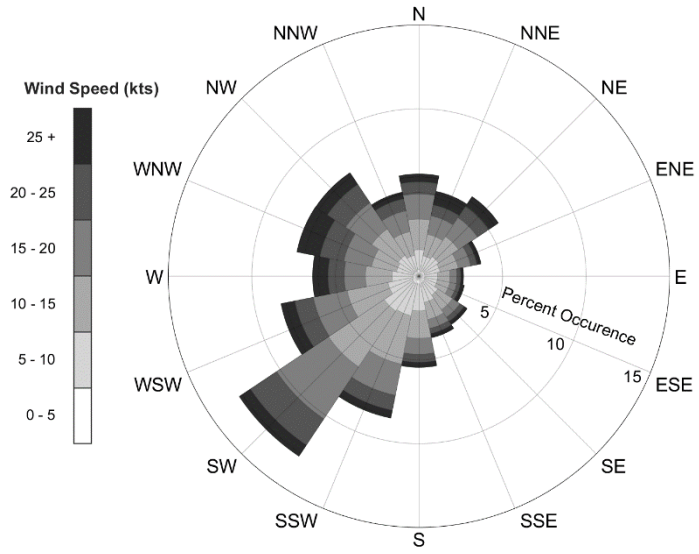

Figure 3.7 Continuous wind data collected from the NDBC C-MAN station BUZM3 (southwest of Cuttyhunk Island) for the 24-year period between May 1997 and present. Direction indicates from where the wind was blowing. Wind speeds are color coordinated such that larger magnitudes correspond to darker gray tones. Wind speeds are color coordinated such that larger magnitudes correspond to darker gray tones. Combined length of segments in each sector indicates percent occurrence of wind speeds from that direction.

3.3 Historic Storms and Sea Level Rise

Historical water level data were obtained from the National Oceanic and Atmospheric Administration (NOAA) water level and tide station in Woods Hole (Station 8447930), located approximately 7 miles southwest of Eel River Inlet. Tide datums (Table 3.5) and mean tide range (1.79 feet) for the Woods Hole gauge station show strong similarity to the datums and mean tide range measured at the offshore tide gauge for Eel River Inlet (1.71 feet), providing a comparable source of historical water levels that have been experienced in the area. The Woods Hole water level dataset includes 90 years of water level data, spanning the time period between 1932 and the present date (Figure 3.8a). Major tropical storms such as the hurricanes of 1938, 1944, 1954 (Carol), and 1991 (Bob) exhibit a much stronger influence on extreme water levels rather than extra-tropical storms (nor'easters). Typically, tropical storms pass through the area over a period of less than 6 hours and can generate modest short-period storm waves and relatively large storm surge. The aforementioned tropical storms all produced storm-driven water levels exceeding the calculated benchmark for a 10-year return period storm, whereas even severe extra-tropical storms have all recorded water levels with return periods below the 10-year event. A full depiction of the annual exceedance probability curve for the Woods Hole tide gauge is shown in Figure 3.8b.

Although the return period storm surge levels provided in the most recently revised Flood Insurance Study for Barnstable County (FEMA, 2021) correspond well with the statistical analysis calculated using the water elevation record from Woods Hole, an increasing deviation in values can be seen for decreasing storm return probability (Table 3.6). Specifically, the recorded data suggest storm surge levels for the 50- and 100-year storms are less than predicted by FEMA by 1.2 and 2.8 feet, respectively.

While return period water levels calculated based on the tide gauge record correspond relatively well with those predicted by FEMA, they do not include wave runup or the movement of water up a slope. Therefore, resulting in lower values than the Base Flood Elevations (BFE) defined by FEMA which are the basis for the National Flood Insurance Program (Figure 3.9). However, the 100-year surge levels predicted by FEMA and those calculated from the Woods Hole tide gauge are still capable of washing over the low-lying barrier spit adjacent to Eel River Inlet as well as inundating nearby coastal properties. Figure 3.10 shows water depths in the vicinity of Eel River Inlet caused by a 100-year storm surge predicted by FEMA.

Table 3.5 Tide datums for the Offshore tide gauge at Eel River

Tide Datum	Offshore (ft, NAVD88)
Maximum Tide	9.42
MHHW	0.84
MHW	0.56
MTL	-0.33
MLW	-1.23
MLLW	-1.36
Minimum Tide	-4.63

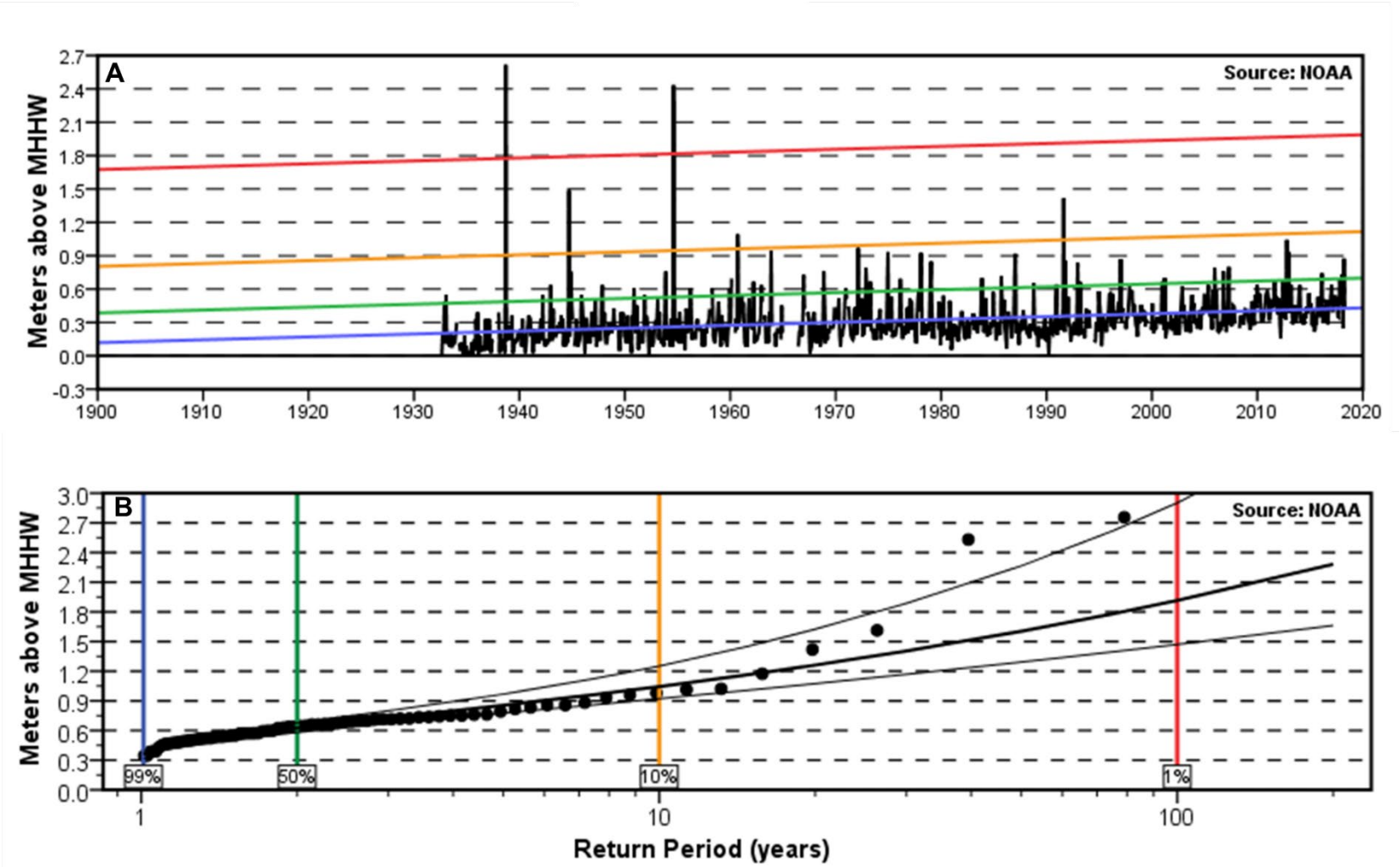

Figure 3.8 Extreme water levels (A) and annual exceedance probability (B) recorded from the Woods Hole tide gauge (Station 8447930). (Credit: provided by NOAA CO-OPS)

Table 3.6 Return period stillwater elevations predicted by FEMA and calculated from data record for NOAA Woods Hole tide gauge station.		
Return Period	FEMA Predicted Stillwater Elevation (ft, NAVD88)	NOAA Recorded Stillwater Elevation (ft, NAVD88)
10-Year (10-percent annual chance flood)	4.5	4.5
50-Year (2-percent annual chance flood)	8.1	6.9
100-Year (1-percent annual chance flood)	10.1	7.3
500-Year (0.2-percent annual chance flood)	14.9	NA
*The Effective FEMA Flood Insurance Study and Maps for Barnstable County were revised on July 6, 2021		

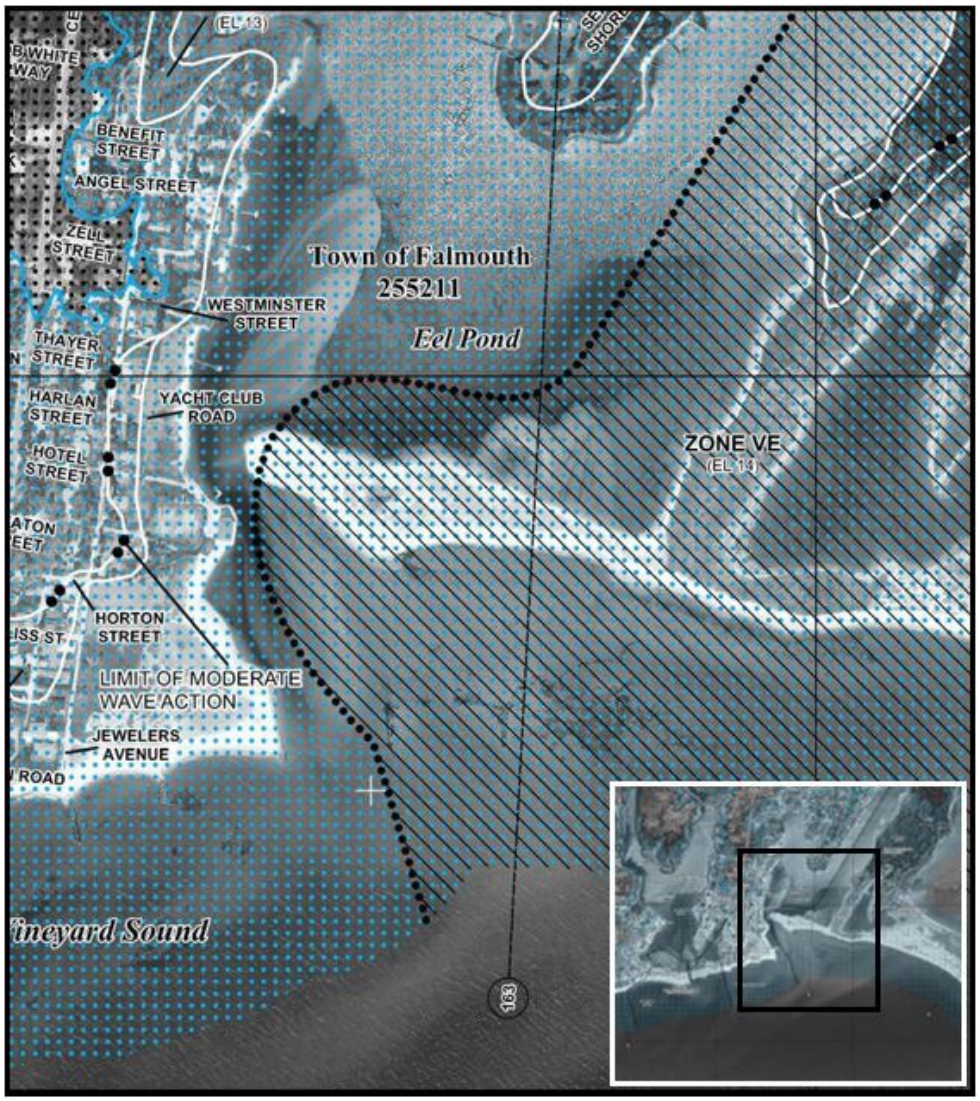

Figure 3.9 FEMA Flood Insurance Rate Map (FIRM) for the vicinity of the project area (inset: FEMA sheet 25001C0741J).

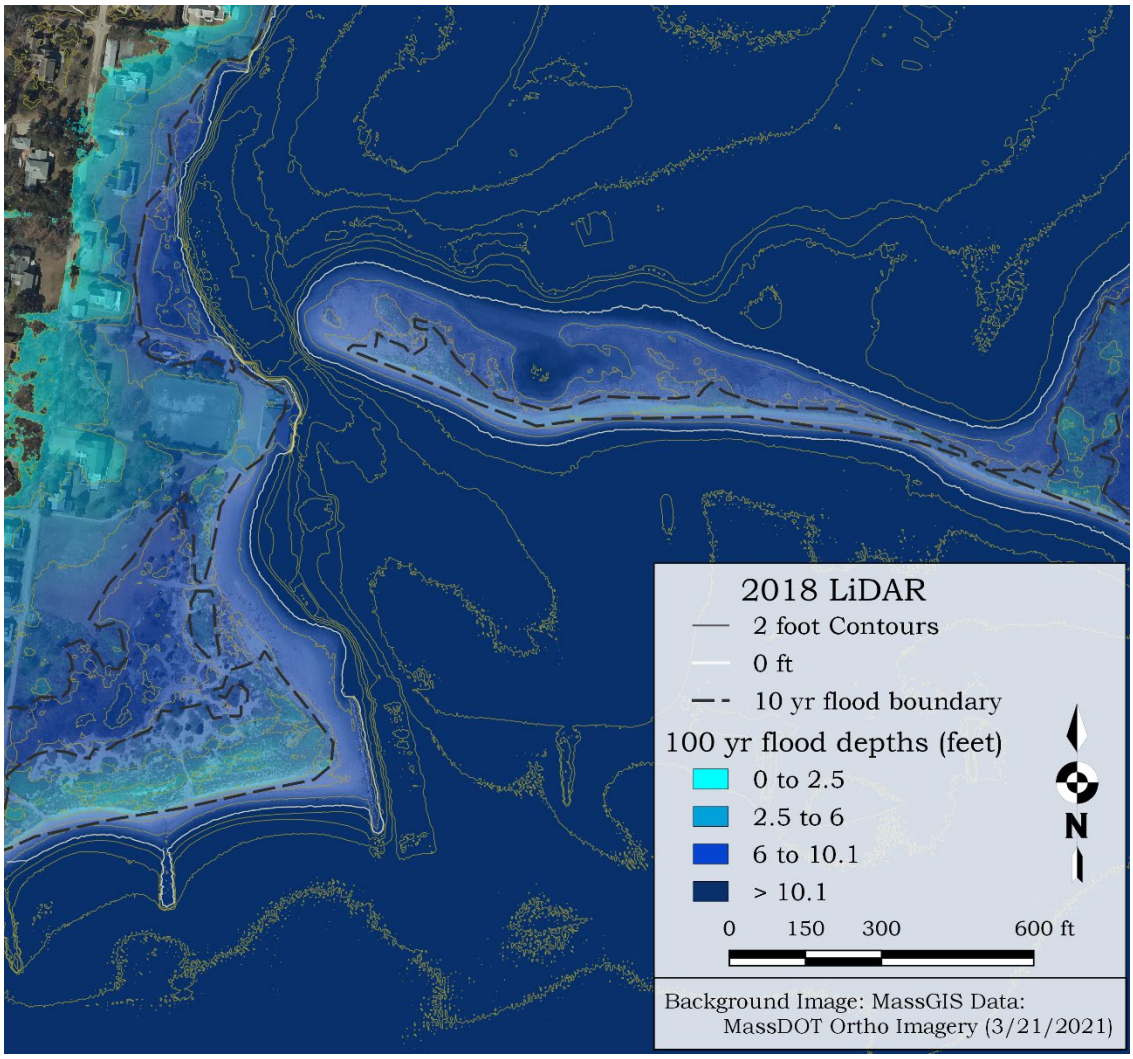

Figure 3.10 Map of the Eel River inlet entrance channel and Washburn Island barrier spit impacted by a FEMA 100-year storm with still water levels of over 10.1 feet NAVD88. With sea-level rise, a flooding event equivalent to the 100-year flood will occur more frequently. The significant storm elevation of 4.5 feet was determined by FEMA to be the elevation of the 10% annual chance flood elevation.

Most of the barrier beaches on Cape Cod are “transgressive,” i.e., migrating landward and upward (in the long-term) to cover the water body or salt marsh that lies behind it. This process is driven by sea level rise and overtopping due to infrequent large storm events; the barrier beach migrates to maintain equilibrium with the changing environment. While the rapidly changing inlet and barrier beach morphology is the primary driver to erosion problems along the shoreline adjacent to Eel River Inlet, sea level rise and associated impacts of higher storm surge levels will exacerbate evolution of the barrier beach system and increase potential risks to public safety, coastal infrastructure, and natural resources.

Separate from the daily rise and fall of the tide, the average elevation of the ocean changes over time with respect to the land. This average position is called relative sea level and different geologic and atmospheric processes contribute to changes in relative

sea level. Some of the causes include glacial ice melt, thermal expansion of the ocean as the global temperature increases, the velocity of the offshore Gulf Stream current, and the rising or sinking of the earth's crust itself. While the specific causes and future amounts of relative sea level rise (SLR) are the topic of much scientific debate, historical and present rates of SLR are well known for the region. Historical evidence indicates that over the past 90 years the relative sea level in Woods Hole, Massachusetts has been rising generally in a linear fashion, with an average rate of approximately 0.118 inches per year or 0.98 feet per century (Figure 3.11).

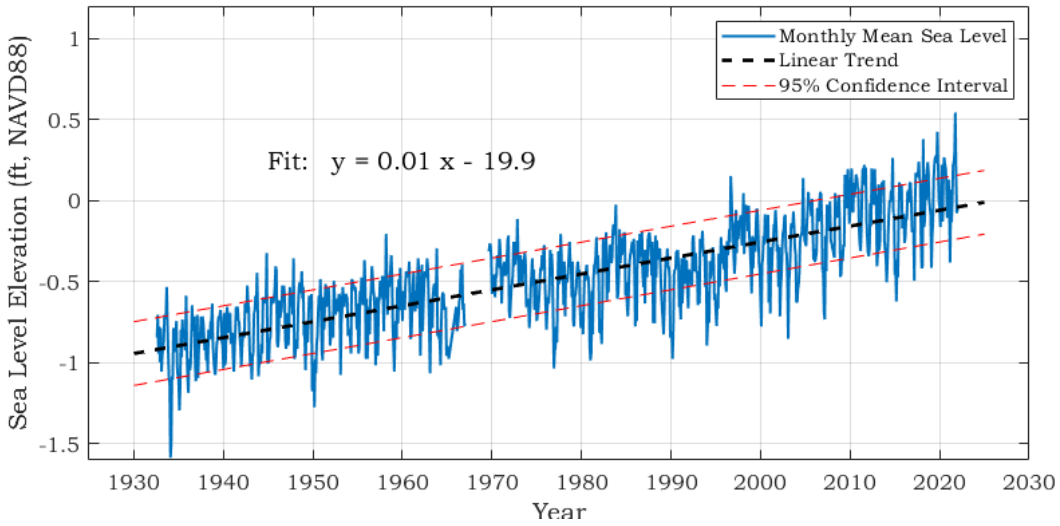

Figure 3.11 Monthly mean water levels recorded in Woods Hole between 1932 and 2021 indicate a linear trend in sea level rise over the past 90 years of approximately 0.01 feet per year.

While long-term tide records (e.g. Woods Hole) provide valuable insight into historical changes over the past century, they do not necessarily dictate future response of sea level rise due to changing environmental and anthropogenic conditions. Predictive models have been developed and calibrated to forecast the effects of climate change on relative sea level rise in coming decades. New and existing models used to predict sea level rise are continually refined with augmented datasets to reduce output uncertainty, however there still exists a large range of potential sea level rise scenarios.

Based on the Massachusetts Sea Level Assessment and Projections technical memorandum (DeConto and Kopp, 2017) regarding local mean sea level rise, plots were developed for the Commonwealth of Massachusetts to provide guidance regarding future predictions of sea level rise in Woods Hole (Figure 3.12). The range of varying projections are determined based on the probability of exceedance given two future atmospheric greenhouse gas concentration pathways, medium (RCP4.5) and high (RCP8.5; Van Vuuren et al., 2011), and for two methods of accounting for Antarctic ice sheet projections: one based on expert elicitation (Kopp et al., 2014) and one where Antarctic ice sheet projections are driven by new, process-based numerical ice sheet model simulations (DeConto and Pollard, 2016; Kopp, 2017). These localized projections are downscaled from regional and international projections, where the intermediate SLR estimates were consistent with the International Panel on Climate Change (IPCC), the 2017 National Climate Assessment, and the Global and Regional Sea Level Rise Scenarios for the

United States (NOAA). A brief description of the probabilistic projections is provided in Table 3.7.

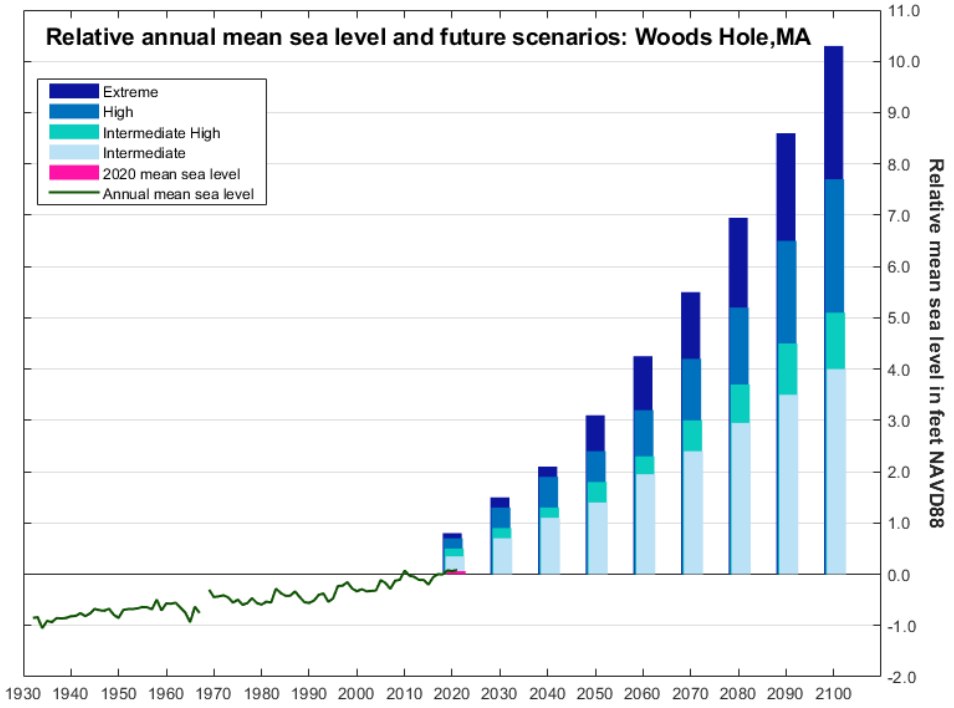

Figure 3.12 Relative mean sea level projections for the Woods Hole, MA tide station based on four National Climate Assessment global scenarios with associated probabilistic model outputs from the Northeast Climate Science Center. The probabilistic projections are listed in Table 3.7. The pink bar denotes the 2020 recorded mean sea level in Woods Hole. The green curve represents the annual mean sea level calculated from the data record presented in Figure 3.11.

Table 3.7 Relative mean sea level (feet, NAVD88) projections for Woods Hole, MA

Scenario	Probabilistic projections	2030	2050	2070	2100
Intermediate	Unlikely to exceed (83% probability) given a high emissions pathway (RCP 8.5)	0.6	1.3	2.3	4.0
Intermediate - High	Extremely unlikely to exceed (95% probability) given a high emission pathway (RCP 8.5)	0.8	1.7	2.9	5.1
High	Extremely unlikely to exceed (99.5% probability) given a high emission pathway (RCP 8.5)	1.1	2.4	4.2	7.7
Extreme (Maximum physically plausible)	Exceptionally unlikely to exceed (99.9% probability) given a high emissions pathway (RCP 8.5)	1.3	3.1	5.4	10.3

Accurate projections of sea level rise are critical for engineers and coastal managers developing future coastal hazard mitigation and improvement alternatives. Enhanced precision in the prediction of future storm driven flood and tidal elevations ensures the consideration of sufficient safety measures while also maintaining economic feasibility and reducing the potential of adverse environmental impacts. Using the recorded water elevations measured in Woods Hole for 2020, a direct comparison between measured and projected relative sea level can be evaluated to assess the accuracy of the most up-to-date modelling projections (Figure 3.13). The results of this assessment indicate that sea level projections over the first decade, when utilizing the recommended "high scenario", are overestimated by approximately an order of magnitude. Figure 3.14 shows annual mean levels and future sea level rise projections for Boston Harbor used as an example to refine the scope of possible sea level rise scenarios. The 'extreme' projection was adjusted to account for the calculated offset between the 2020 projection and the recorded annual mean sea level. Additionally, predictions published by the Intergovernmental Panel on Climate (IPCC, 2013), modified to account for estimates of sea level rise acceleration contributions from Greenland and Antarctic ice sheets based on data collected between 1992 and 2009 (Rignot et al., 2011), were used to corroborate the probabilistic predictions made by DeConto and Kopp (2017; Figure 3.14). Understanding that sea level rise predictions over the next 80 years, with a reasonable probability, range from a linear increase of 0.8 feet (low approximation) to a more rapid exponential increase of 9.5 feet (adjusted 'extreme' approximation), flood mitigation strategies should be determined based on the anticipated design life and relative importance and functionality of the infrastructure subject to improvement.

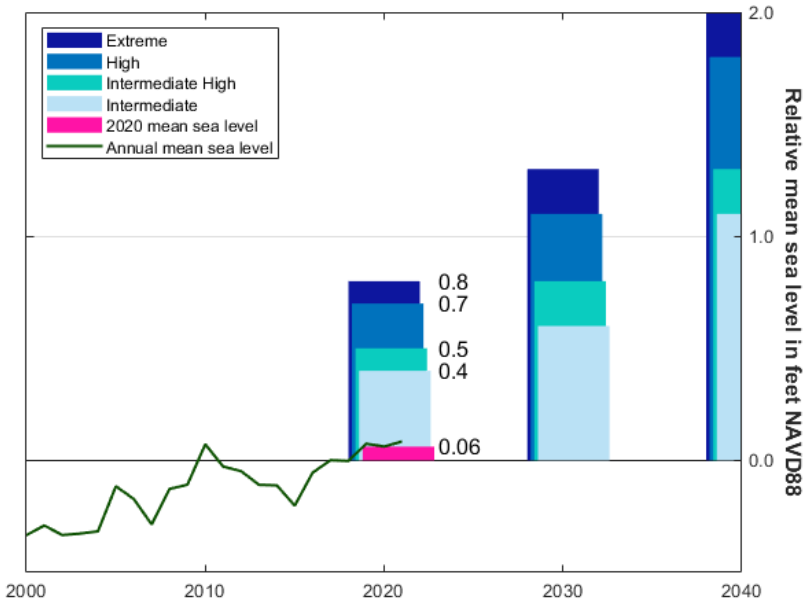

Figure 3.13 Comparison of probabilistic sea level rise projections and measured annual mean sea level for Woods Hole, Massachusetts.

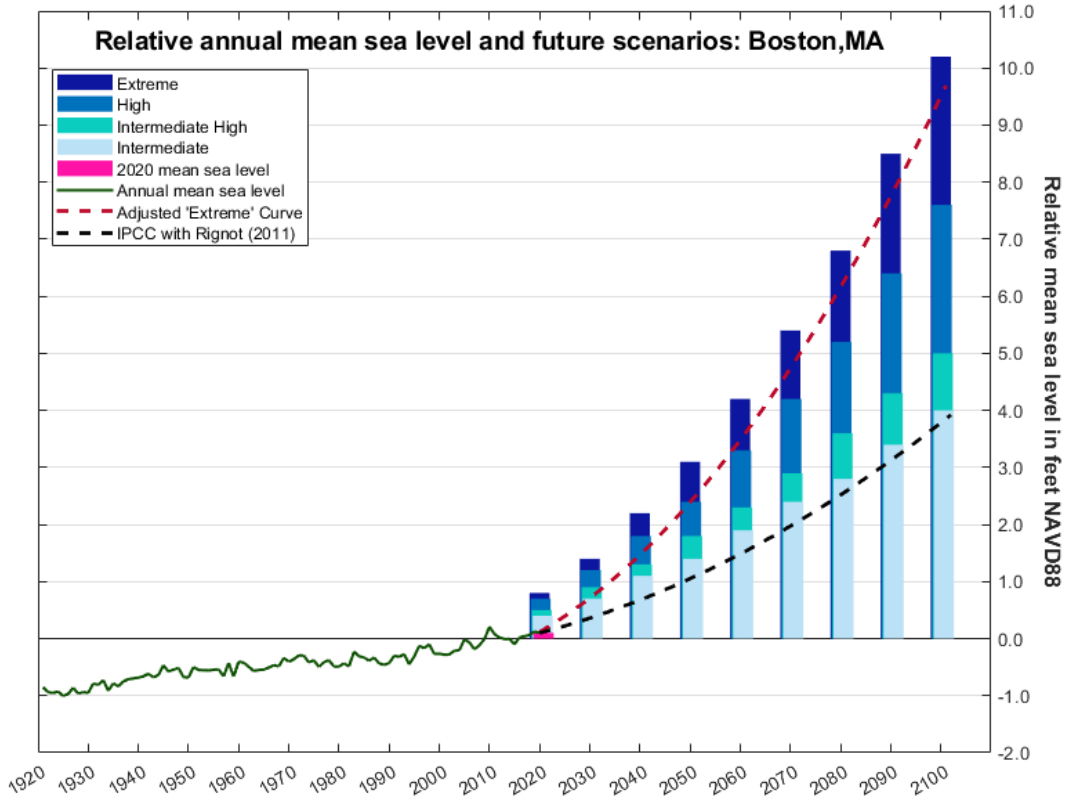

Figure 3.14 Sea level rise predictions with a curve fit to the 'extreme' scenario (adjusted to account for current mean sea level; dashed red line) and a curve representing flood predictions from the IPCC augmented by sheet ice contributions determined by Rignot et al. (2011; dashed black line).

4 HYDRODYNAMIC MODEL

A hydrodynamic model of the Waquoit Bay system was developed and calibrated using tidal data available from the 2013 Massachusetts Estuaries Project (MEP) water quality report for the Waquoit Bay and Eel River embayment system (Howes et al., 2013) in order to investigate the change in hydrodynamic conditions that may result from the proposed alternatives. These data include tidal elevations from 2002 and updated 2018 bathymetric LiDAR data used in conjunction with bathymetric survey data used in MEP water quality report.

4.1 Model Development

For modelling of the Waquoit Bay system, Sustainable Coastal Solutions utilized a state-of-the-art computer model to evaluate tidal circulation. The particular model employed was the Delft 3D Flow FM hydrodynamics model. Flow FM is a flexible mesh, finite volume code that includes a morphologic model than can simulate tidally driven sediment transport and morphology change. Flow FM is an advanced code that can solve

three-dimensional hydrodynamics and sediment transport. The model utilizes a grid mesh that can be constructed using a variety of polygonal elements, with up to six sides. This allows for easy construction of model grids that conform well to complex shorelines and sinuous channels and that can include high degrees of mesh resolution in areas only where it is desired. Sub-grid-scale flow modifying structures such as weirs and thin dams can be specified for the model runs. Combined with Delft 3D Wave, it can be implemented as a fully integrated wave, hydrodynamic, and morphological model.

A flexible mesh grid was generated to cover the entire Waquoit Bay system to ensure flow dependencies between Waquoit Bay and the Eel River estuary via the Seapit River are considered, as well as providing adequate coverage to include all of the significant tidal collection locations used in the 2013 MEP analysis. The full extent of the complete hydrodynamic model grid is represented in Figure 4.1. The model includes tidal open boundaries offshore of the Eel River and Waquoit inlets. The offshore lateral boundaries are configured as Neumann gradient boundaries that allow the development of longshore currents in the offshore area of the grid.

The flexible mesh grid was utilized to increase the model resolution within confined waterways and particular areas of interest such as Eel River Inlet. A close up of the grid focused on the Eel River Inlet and Washburn Island spit is shown in Figure 4.2. The minimum grid cell edge length is approximately 10 feet, with grid cell dimensions increasing offshore and into more wide regions of the embayment system.

A composite bathymetry dataset was interpolated to the model mesh (Figures 4.3 and 4.4). This bathymetry dataset is primarily based on the 2018 USACE Topobathy LiDAR survey for the East Coast. Bathymetric transects surveyed for the MEP water quality project were used to supplement gaps in the LiDAR located in some of the upper regions of the embayment system and NOAA historical GEODAS survey data were used in the offshore region beyond the extent of the LiDAR surveys.

The model was run using a variable time step that is determined based on the metrics of the model stability (courant number, based on velocity, water depth and grid cell size). The maximum model time step was set at 30 seconds, but could be reduced at times when the courant number calculated for the grid cells exceeds the threshold value of 1.

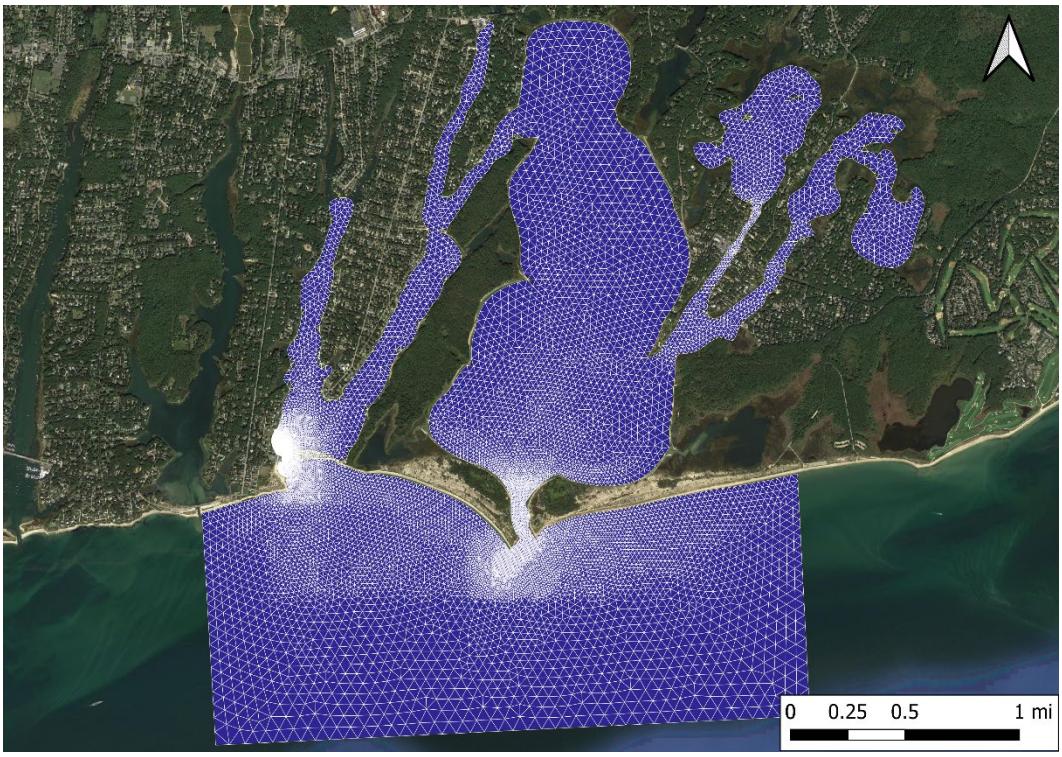

Figure 4.1 Hydrodynamic model mesh of the Waquoit Bay system.

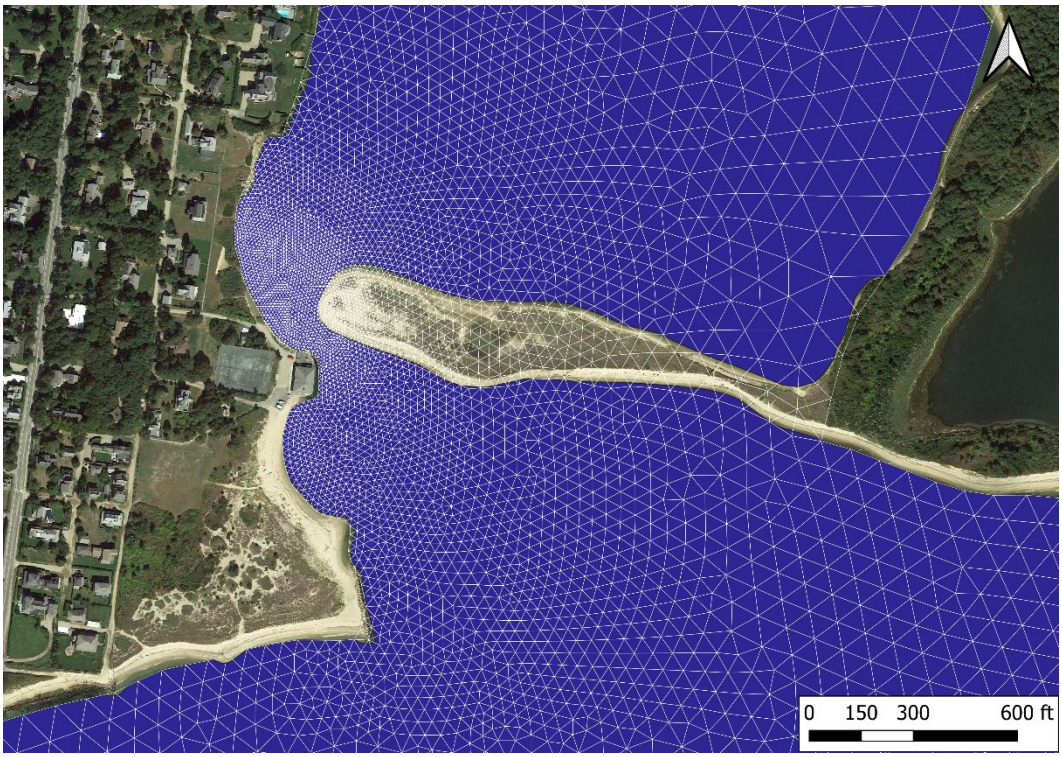

Figure 4.2 Detail of the inlet and the Washburn Island region of the Waquoit Bay hydrodynamic model grid.

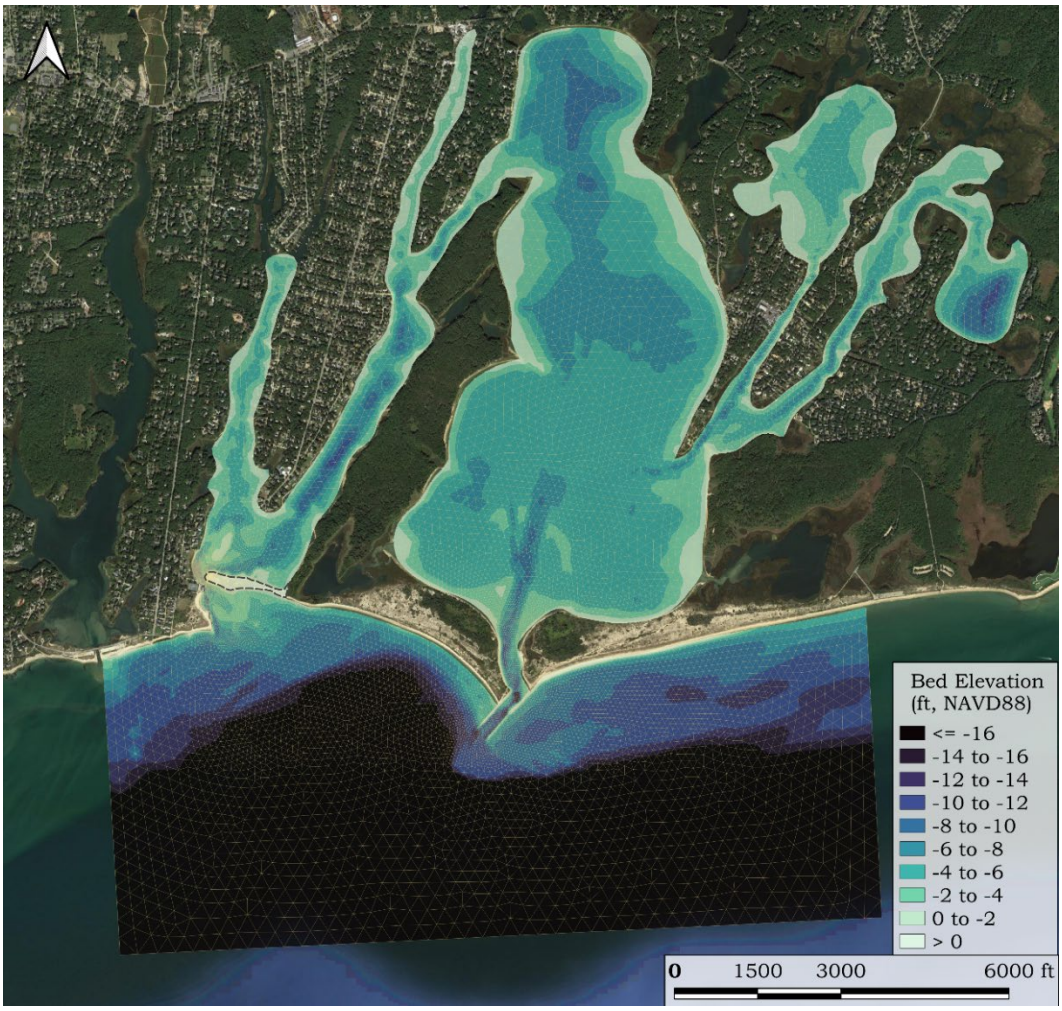

Figure 4.3 Full coverage of the model mesh of the Waquoit Bay system, with color contours of grid bathymetry.

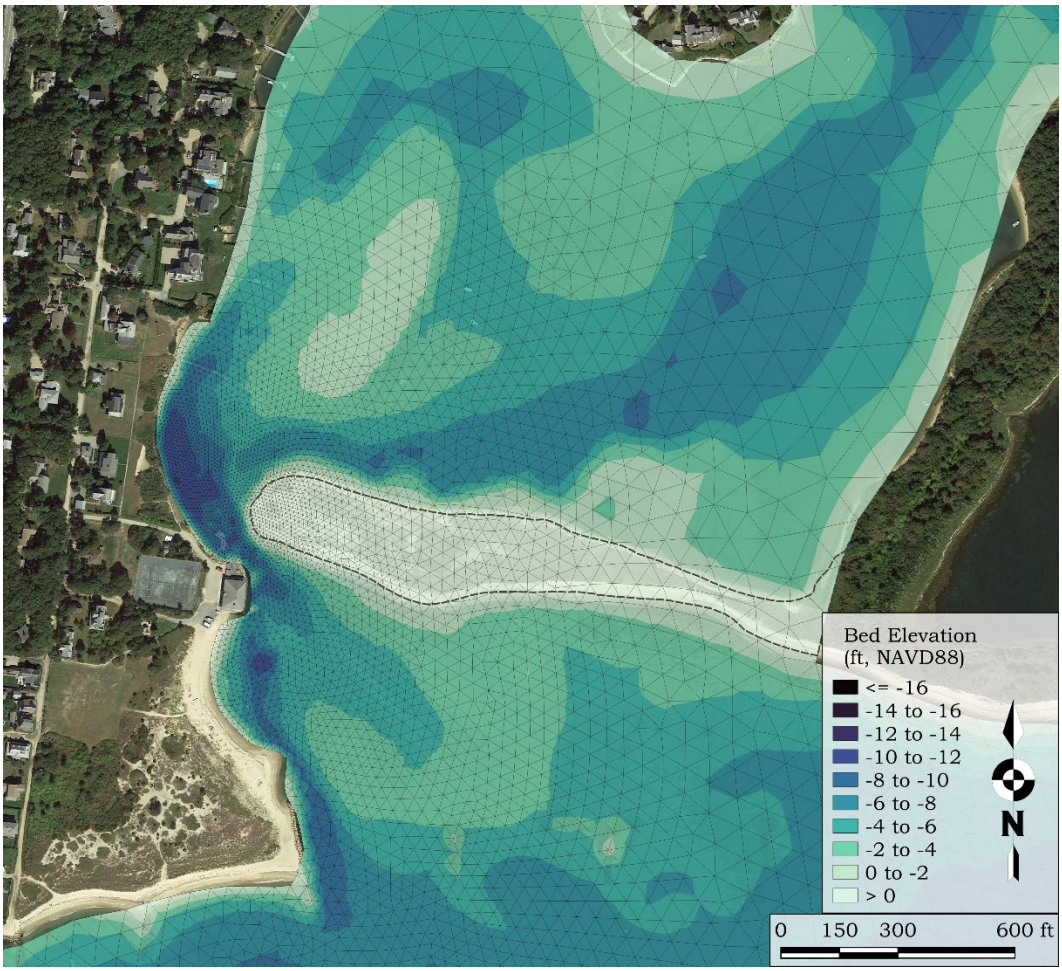

Figure 4.4 Zoomed in bathymetry in the vicinity of Eel River Inlet.

4.2 Model Calibration

After developing the computational grid, and specifying boundary conditions, the hydrodynamic model for the Waquoit Bay system was calibrated. The calibration procedure ensures that the model predicts accurately what was observed in nature during the field measurement period between January 18, and February 19, 2002. Numerous model simulations are typically required for an estuary model, specifying a range of friction and eddy viscosity coefficients, to calibrate the model.

During the process of calibration, values of friction coefficients (Mannings coefficient was used) specified for the entire model domain were varied. Friction inhibits flow along the bottom of estuary channels or other flow regions where velocities are relatively high. Friction is a measure of the bottom roughness and can cause both significant amplitude attenuation and phase lags of the tidal signal. The varied friction coefficients were chosen to replicate the values used in the MEP, and are summarized in Table 4.1. The extents of the different regions of the Waquoit Bay system within the model domain are shown in Figure 4.5.

Table 4.1	Mannings Roughness coefficients used in simulations of modeled embayment system. These embayment delineations correspond to the primary regions denoted in the MEP Water Quality Report.

System Regions	Bottom Friction
Offshore	0.025
Eel River West	0.027
Childs River	0.026
Seapit River	0.027
Waquoit Bay	0.027
Hamblin Pond	0.035
Great River	0.035

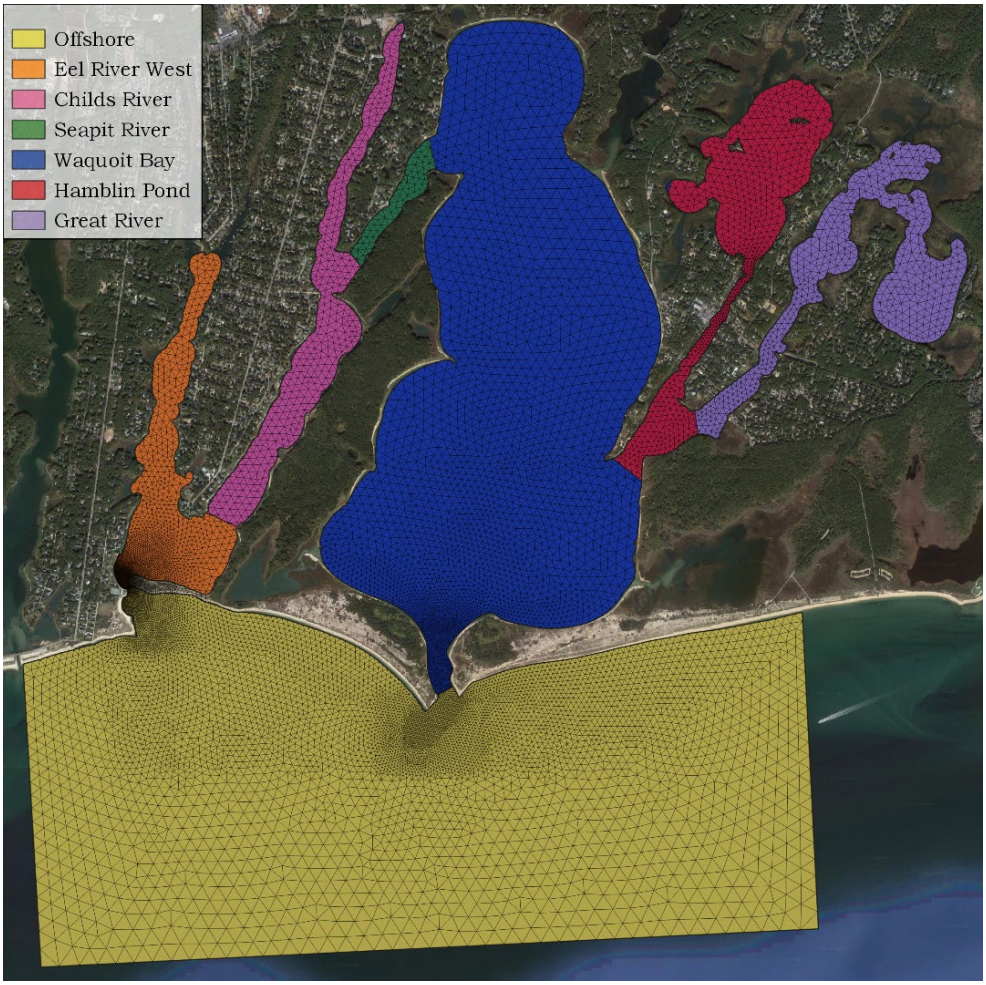

Figure 4.5 Extent of the regions listed in Table 4.1 with the hydrodynamic model grid.

Calibration of the hydrodynamic model required a close match between the modeled and measured tides in each of the embayment regions where tides were measured. Initially, the model was calibrated to obtain visual agreement between modeled and measured tides. Once visual agreement was achieved the model output was evaluated and compared to the measured tide data through the tidal constituent analysis discussed in Section 3.1. Tide constituents for both modeled and measured tides were evaluated to ensure proper phasing and amplitude of tide across the Waquoit Bay system. The comparison of modelled and measured tides is presented in Figures 4.6 and 4.7, and in Table 4.2. The calibration shows the considerable skill of the model with constituent amplitude errors that of the order of 10^{-2} feet, and phase errors that are generally (with the exception of Hamblin Pond) equal to the magnitude of the time step associated with the measured tide data (approximately 10 minutes). The relatively large phase errors observed in Hamblin Pond were expected due to coarsely resolved grid spacing in Little River and the lack of consideration for supplemental flushing through the creek north of Seconsett Island. due to the negligible effects this region of the system would have on the hydrodynamics of Eel River Inlet.

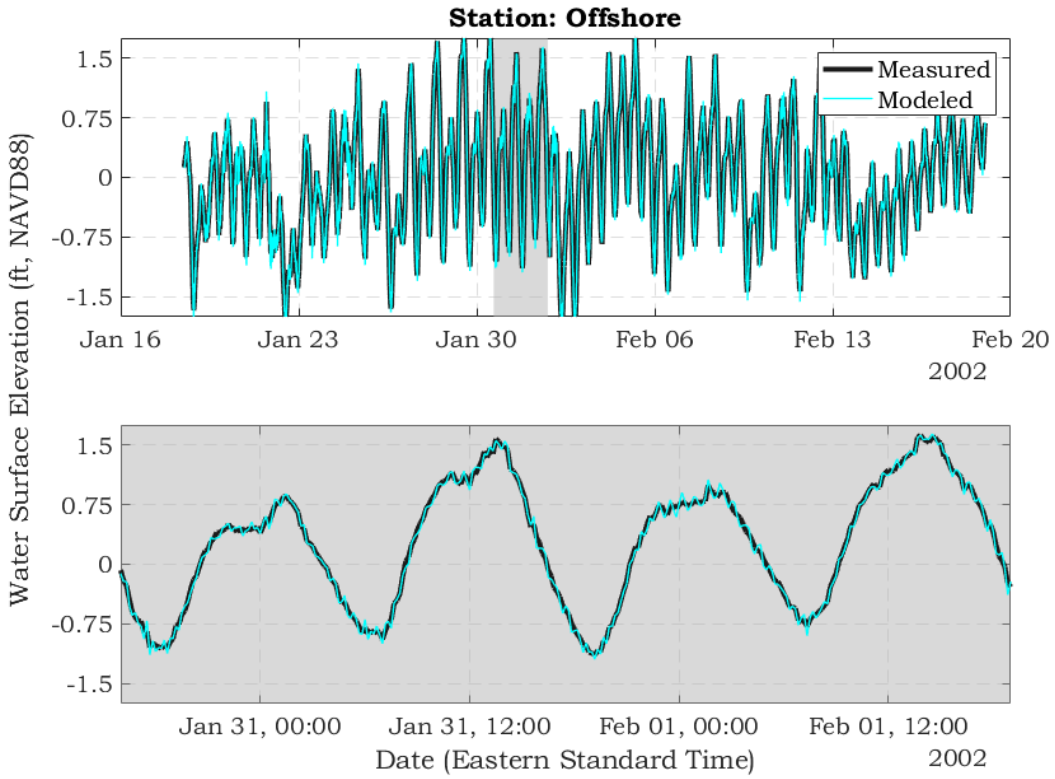

Figure 4.6 Comparison of measured and modeled tides at the Offshore station of the Waquoit Bay system. The lower figure represents a zoomed in view of the gray-shaded area from the upper figure.

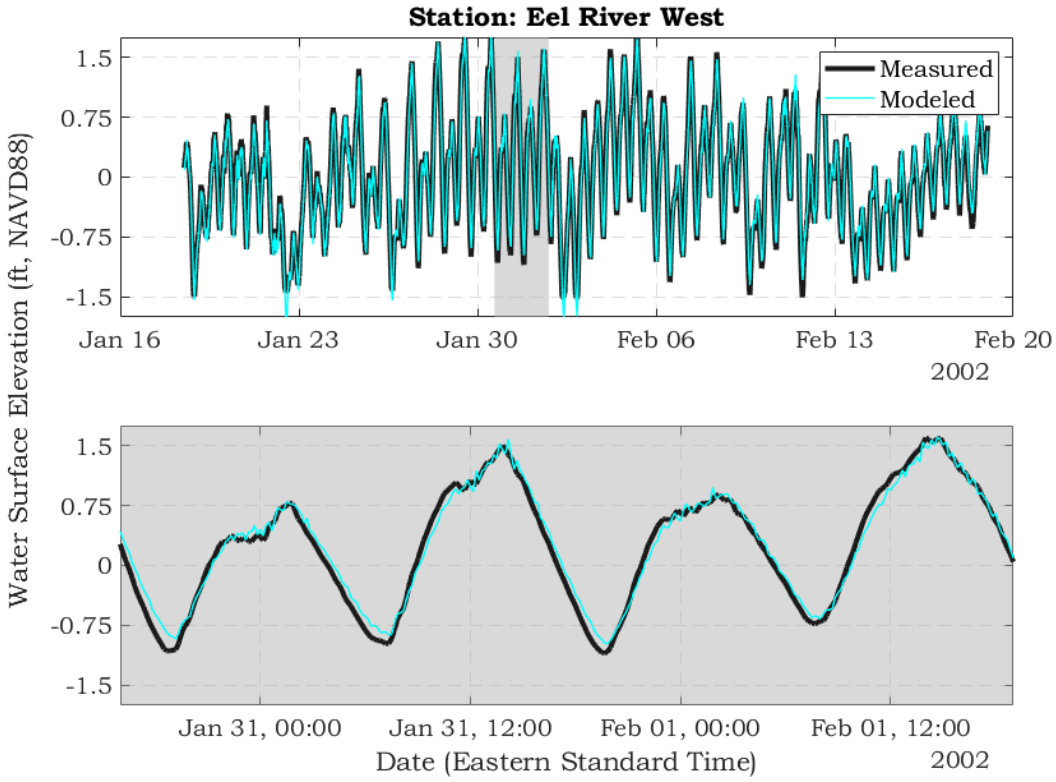

Figure 4.7 Comparison of measured and modeled tides at the Eel River West station of the Waquoit Bay system. The lower figure represents a zoomed in view of the gray-shaded area from the upper figure.

Table 4.2 Tidal constituents for measured water level data and calibrated model output, with model error amplitudes, for the Waquoit Bay system.

Measured Tide						
Location	Constituent Amplitude (ft)				Phase (deg)	
	M_2	M_4	M_6	K_1	φM_2	φM_4
Offshore	0.68	0.16	0.05	0.24	82.40	-59.95
Eel River	0.66	0.13	0.06	0.26	93.72	-36.39
Childs River	0.64	0.11	0.05	0.24	98.62	-25.87
Waquoit Bay	0.64	0.09	0.04	0.24	104.95	-12.80
Hamblin Pond	0.63	0.07	0.05	0.24	117.57	22.14
Great River	0.65	0.09	0.05	0.24	113.59	11.01
Modeled Tide						
Location	Constituent Amplitude (ft)				Phase (deg)	
	M_2	M_4	M_6	K_1	φM_2	φM_4
Offshore	0.68	0.16	0.05	0.24	82.59	-60.21
Eel River	0.63	0.11	0.05	0.24	98.89	-28.94
Childs River	0.63	0.09	0.05	0.24	103.75	-17.29
Waquoit Bay	0.61	0.07	0.04	0.23	109.88	-8.40
Hamblin Pond	0.58	0.02	0.03	0.23	129.37	60.41
Great River	0.61	0.05	0.04	0.23	118.64	18.06
Error (measured - modeled)						
Location	Amplitude Error (ft)				Phase Error (minutes)	
	M_2	M_4	M_6	K_1	φM_2	φM_4
Offshore	0.00	0.00	0.00	0.00	-0.40	0.26
Eel River	0.03	0.02	0.01	0.02	-10.70	-7.72
Childs River	0.02	0.03	0.00	0.00	-10.61	-8.88
Waquoit Bay	0.03	0.02	0.00	0.01	-10.21	-4.56
Hamblin Pond	0.05	0.05	0.01	0.01	-24.42	-39.62
Great River	0.04	0.04	0.01	0.01	-10.46	-7.30

The final calibrated model serves as a useful tool in investigating the circulation characteristics of the system. Using model inputs of bathymetry and tide data, current velocities and flow rates can be determined throughout the model domain. This is a very useful feature of a hydrodynamic model, where a limited amount of collected data can be expanded to determine the physical attributes of the system in areas where no physical data record exists.

Evaluation of the results from the model run of the Waquoit Bay system shows the maximum flow velocities occur in the inlet channels to Waquoit Bay and Eel River. Ebb velocities in Eel River Inlet are slightly larger than velocities during the maximum flood, with an average maximum velocity of 4.82 feet/sec during ebb cycles and 4.26 feet/sec during flood cycles. Whereas in the Waquoit Bay inlet the flood tide velocities are dominant, although the difference between the ebb and flood cycles is less pronounced with average maximum velocities of 2.97 and 2.87 feet/sec during flood and ebb cycles, respectively. A close-up of the model output is presented in Figure 4.8, which shows color-coded velocity magnitude contours along with velocity vectors, which indicate the direction of flow, for a single model time-step, at the portion of the tide where maximum flood velocities occur.

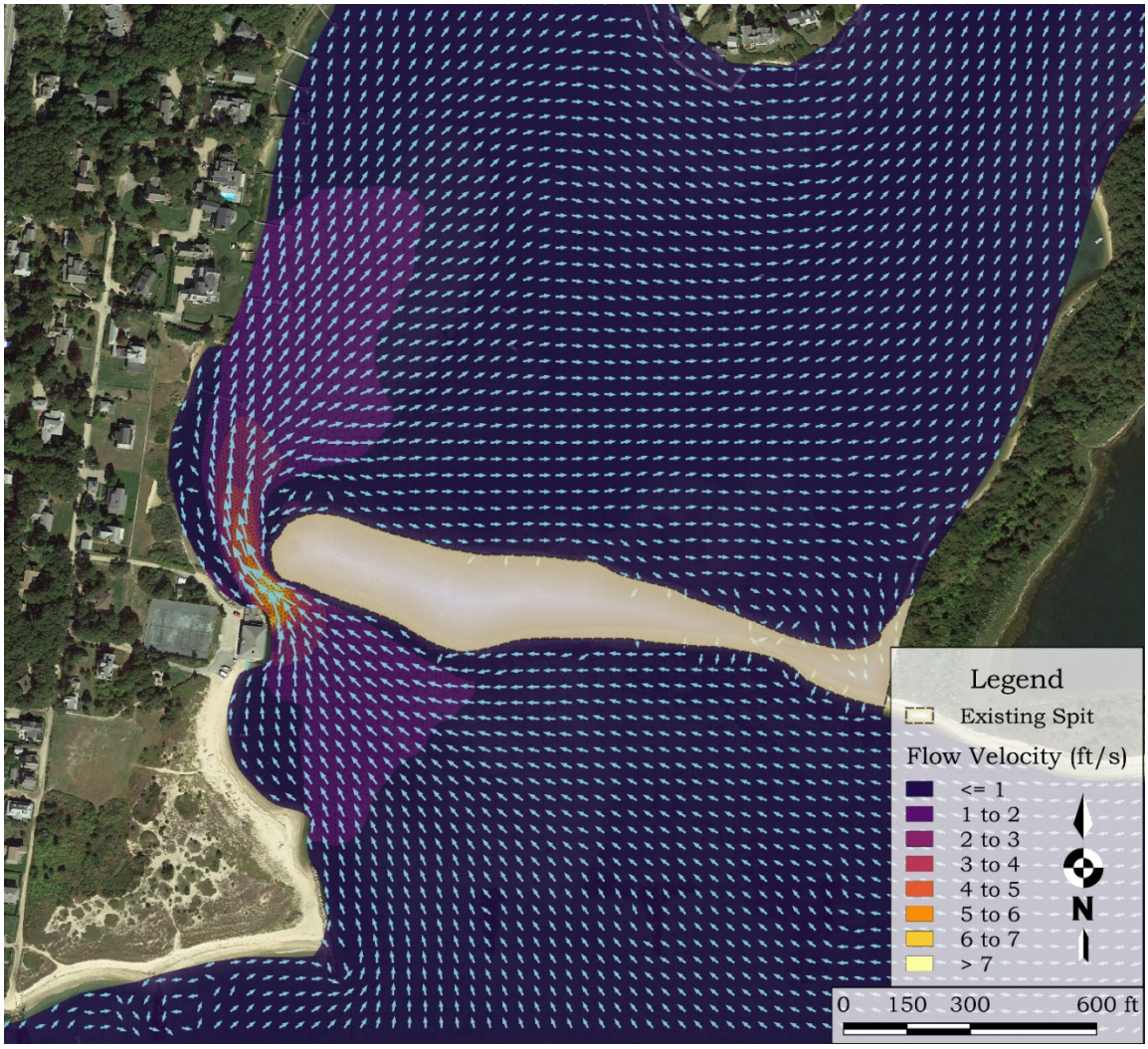

Figure 4.8 Example of hydrodynamic model output with existing conditions for a single time step where typical maximum flood velocities occur. Color contours indicate flow velocity, and vectors indicate the direction and magnitude of flow.

5 WAVE MODEL

As waves propagate into shallower water near shore, the height of the shoaling waves will change, and they will gradually change direction to conform to the bathymetry in that area. In addition, the geography of Nantucket Sound tends to directly block a much of the wave energy propagating from the south due to Marthas Vineyard and Nantucket, which increases the complexity of identifying the specific combination of conditions that influence different regions of the South Cape shoreline. In order to estimate how waves evolve as they propagate toward the south-facing shorelines of the Waquoit Bay system under the influence of winds blowing across the surface of Nantucket Sound, a previously developed two-dimensional wave transformation model, SWAN, was used. Wind data from the BUZM3 NDBC offshore platform and wave data from the WIS hindcast were used as boundary input to the runs of SWAN.

5.1 Model Grid Development

SWAN (an acronym for Simulating Waves Nearshore) is a steady state, spectral wave transformation model developed at the Delft University of Technology of the Netherlands (Booij et al., 1999). Two-dimensional (frequency and direction vs. energy) spectra are used as input to the model. SWAN is able to simulate wave refraction and shoaling induced by changes in bathymetry and by wave interactions with currents. The model includes a wave breaking model based on water depth and wave steepness. Model output includes significant wave height H_s, peak period T_p, and wave direction θ.

SWAN is a flexible and efficient program based on the wave action balance equation that can quickly solve wave conditions in a two-dimensional domain using the iterative Gauss-Seidel technique. For this study, the model was implemented using a steady state finite-difference scheme, on a regular Cartesian grid (computational cell dimensions in the x and y directions are equal), though other options are available (including a finite difference formulation using an unstructured mesh). A great advantage of the iterative technique employed in SWAN it that it can compute spectral wave components for the full 360-degree compass circle.

In addition to the spectral wave boundary conditions specified for each of the wave cases, bathymetry and several model parameters must be specified. The model parameters describe the extent and resolution of the computational mesh (separate from the bathymetry grid) including nested grids, the directional and frequency resolution of the wave spectrum, and wave physics (e.g., breaking, wave-wave interactions).

The SWAN model developed for Eel River Inlet used a coarse grid with 100-meter spacing for the region including the extents of Nantucket Sound and offshore region beyond Marthas Vineyard, Nantucket, and Monomoy Island (Figure 5.1), and a fine nested mesh with a 10-meter spacing that covers the study area around the Eel River and Waquoit Bay inlets (Figure 5.2). The x- and y-axis of the large-scale regional grid are approximately 55 and 35 miles (or 885 and 561 cells) long, respectively. The x-axis is oriented to the east. The greatest depth in the coarse grid domain is -138 feet NAVD88, which occurs at the open boundary. The National Ocean Service (NOS) was the main source of bathymetric data used to create the coarse grid (NOS, 1998). The small-scale grid encompassing Eel River Inlet is made up of 37,901 computational cells spanning approximately 1.5 miles east-to-west and 0.9 miles south-to-north. The bathymetry used

for the nested grid was collected during the 2018 USACE Topobathy LiDAR survey for the East Coast.

The coarse grid was used to propagate offshore waves developed from the analysis of the WIS hindcast record (through Muskeget Channel and over Monomoy shoals), and also generate wind-waves in Nantucket Sound. The nested fine mesh serves to provide detailed wave information at Eel River entrance channel as well as the shorelines north of Menauhant Yacht club and along the southern end of Seacoast Shores. The fine grid model utilizes wave output from the coarse model grid for boundary conditions. As executed, spatially varying model output from the coarse grid (at points that corresponding to nodes along the fine grid open boundary) is used as the boundary condition for the fine grid model runs, therefore the fine grid results are truly nested within the coarse grid simulations.

The wave spectrum resolution specified for the model runs of both coarse and fine model meshes included the full 360-degree compass circle divided into 72, five-degree segments, with 40 discrete frequencies, between 0.05 and 1.00 Hz (corresponding to periods of between 20 and 1.0 seconds).

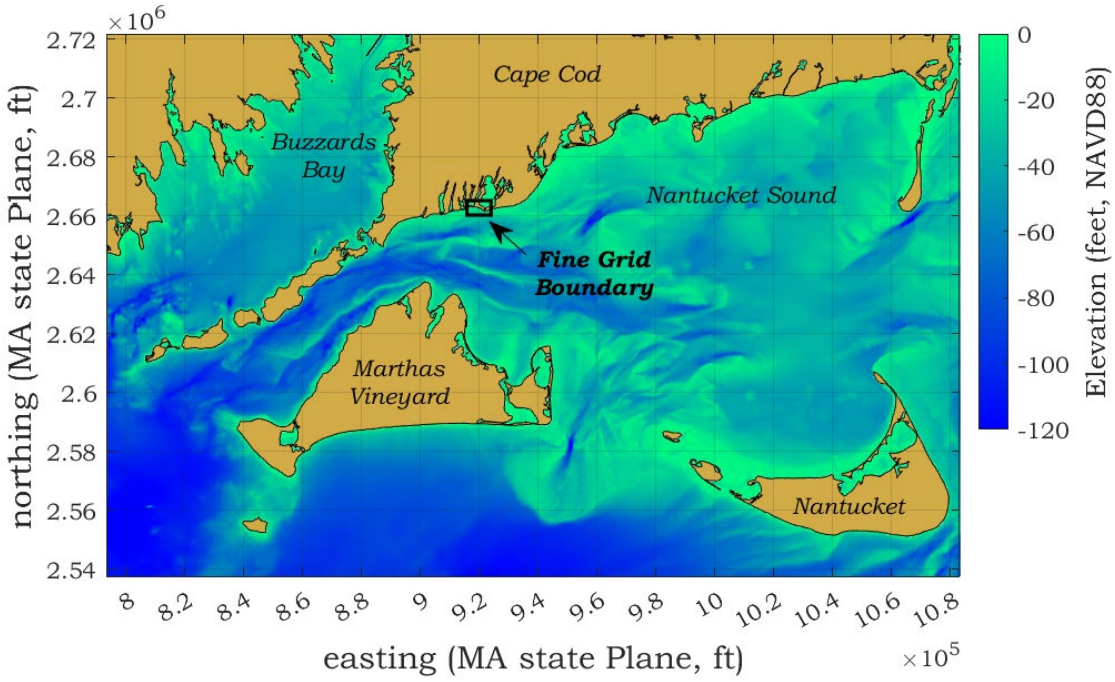

Figure 5.1 Extent of the 2D SWAN wave model grid used to determine wave conditions in Nantucket Sound. The location of the fine model grid for Eel River Inlet is outlined by the black rectangle.

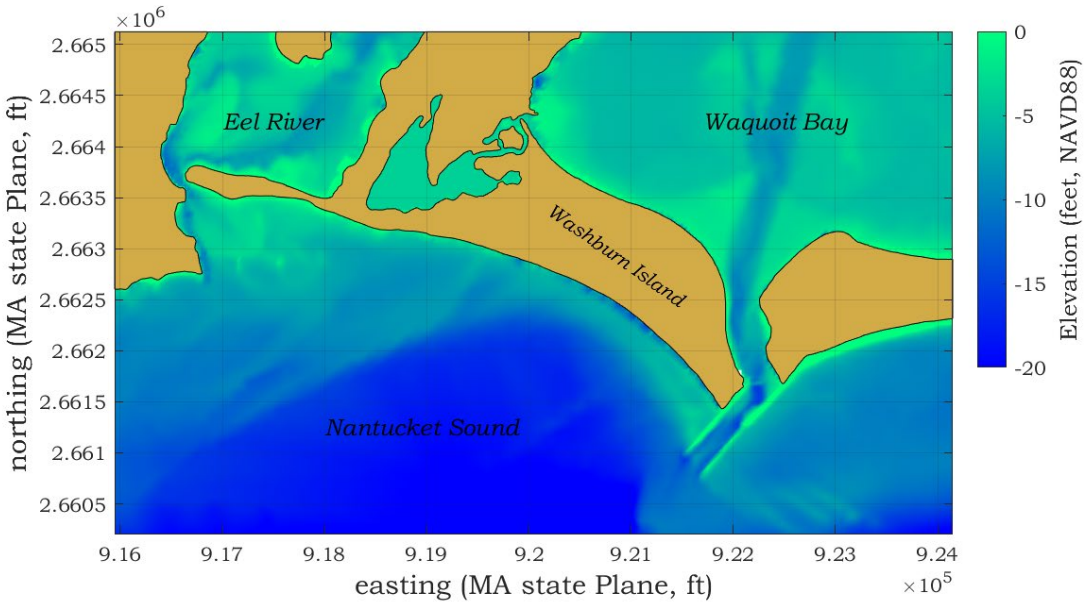

Figure 5.2 Color contour plot showing the limits of the high-resolution fine grid used to model waves approaching Eel River Inlet.

5.2 Model Run Cases Development

Due to the orientation of Eel River Inlet and the focus shorelines, wind waves that have the capability to create potential storm impacts and transport sediment are restricted generally to the south-to-east compass sectors. From this quadrant, three different wind directions (east, southeast, and south) were inspected based on three return periods (1-, 10-, and 100-year return periods). Return periods are used to describe the probability that a particular even will occur in any given year. For example, a 100-year wind speed has a one percent (1/100) probability of occurring this year or any other year. Similarly, a 10-year wind would have a ten percent (1/10) chance of occurring during any year.

The extreme wind speeds and wave parameters used for this analysis were determined by a statistical analysis of the NDBC Buzzards Bay C-MAN station and the USACE WIS hindcast station 63082. These stations were used because they have the longest available data records in the region. The time period covered by these records is long enough to allow their use in the calculation of low frequency of occurrence events such a 100-year storm. The resulting return period wind speeds, wave heights, and mean wave period for the three evaluated sectors are presented in Table 5.1.

Table 5.1	Return period wind speeds (U), significant wave heights (H_s), and corresponding mean wave period (T_m) for east, southeast and south sectors. Wind speeds were determined using BUZM3 wind record and wave data was obtained from USACE WIS hindcast (Station 63082)		
	U (kts)	H_s (ft)	T_m (s)
East			
1-year	32.9	8.2	6.9
10-year	47.1	16.7	9.9
100-year	57.8	23.2	12.6
Southeast			
1-year	33.6	9.2	7.2
10-year	43.9	16.7	9.9
100-year	51.7	22.4	11.9
South			
1-year	34.0	9.7	7.4
10-year	45.7	20.2	11.1
100-year	54.6	28.1	13.9

Although winds from the east exhibit the longest fetch (i.e. overwater distance the wind waves are generated), the shoals just inside Monomoy Island reduce much of the energy within the eastern portion of Nantucket Sound and waves do not propagate directly toward Eel River Inlet. Waves propagating from the east without a directional component from the south are generally blocked by the Waquoit Bay inlet breakwaters, resulting in attenuated wave energy as passing waves diffract around the structures. Prior to analyzing the wave model results, it should be noted that significant storms experienced along the Falmouth shoreline (e.g. storms with a surge in excess of the 10-year event) are tropical storms; therefore the wave conditions evaluated from the southeast are highly unlikely to occur during the water level conditions evaluated in the model domain. Regardless, the Southeast 100-year condition coupled with FEMA predicted 100-year flood elevation of 10.1 feet was chosen to represent the 'worst-case' scenario due the increased exposure of the inlet's western shoreline and the interior of the Eel River Embayment. Additionally, since storms with substantial tidal surges along the south coast of Cape Cod are tropical storms, the duration of the surge is typically just a few hours.

5.3 Wave Model Results

Examples of wave model output are presented in Figures 5.3 and 5.4, from the coarse and fine grids, for the 100-year SE conditions discussed in the previous section. In these plots the color contours indicate wave height and vectors are used to indicate the direction of wave propagation. Specific nearshore wave heights were examined at discrete locations along two shore-parallel transects that run along the shoreline north of Menauhant Yacht Club and around the southern point of Seacoast Shores spanning 225

feet and 175 feet, respectively (Figure 5.5). The results are plotted in Figures 5.6 and 5.7 for the southeast sector model run case.

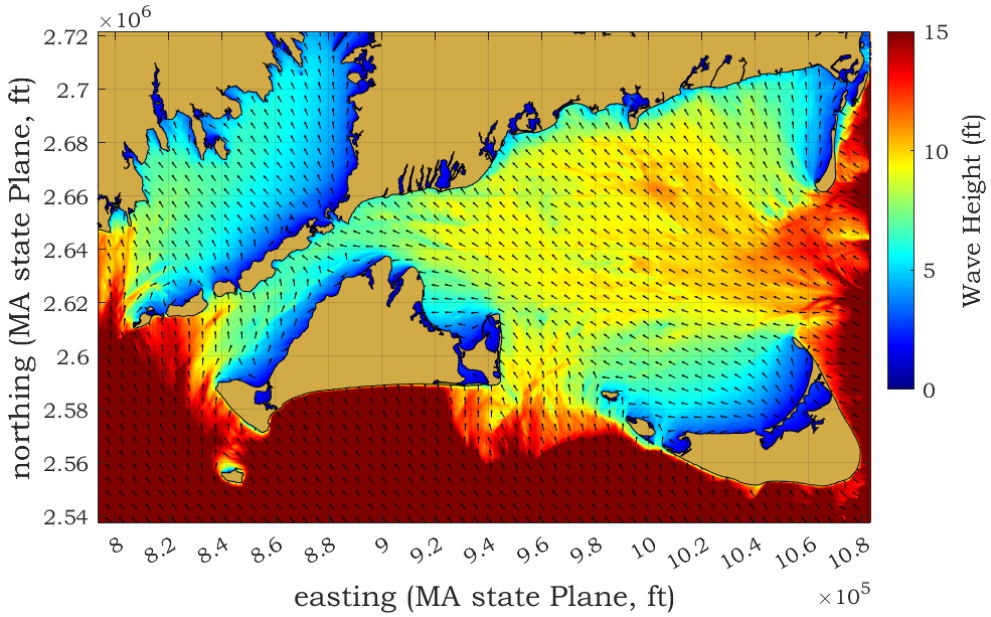

Figure 5.3 Output wave heights from the 2D SWAN wave model for the Nantucket Sound large-scale regional grid, for 100-year (1%) Southeast wind (43.7 kts) and offshore wave conditions (22.4 ft and 11.9 s). Color contours represent significant wave height (H_s), while vector arrows indicate mean wave direction.

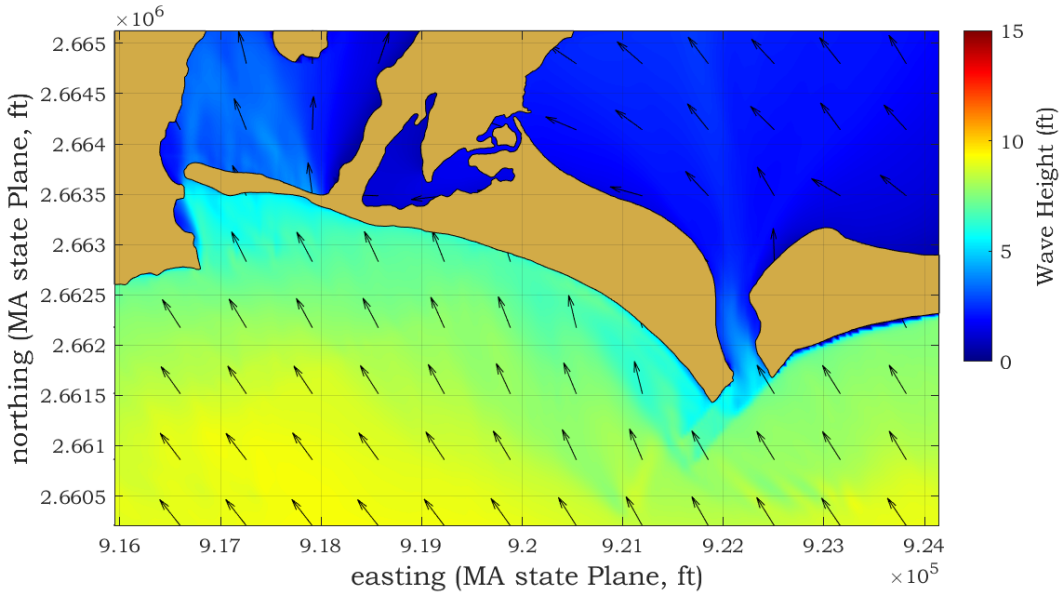

Figure 5.4 Output significant wave height from the 2D SWAN model for the Eel River nested grid, for 100-year (1%) Southeast wind and offshore wave conditions. Wave heights prescribed at the seaward limit of the grid were on average 8.2 feet, based on outputs from the large-scale regional grid.

Figure 5.5 2021 aerial of Eel River Inlet, with shore-parallel transect (with 25-foot stationing) used as the reference line for the plots of wave model results.

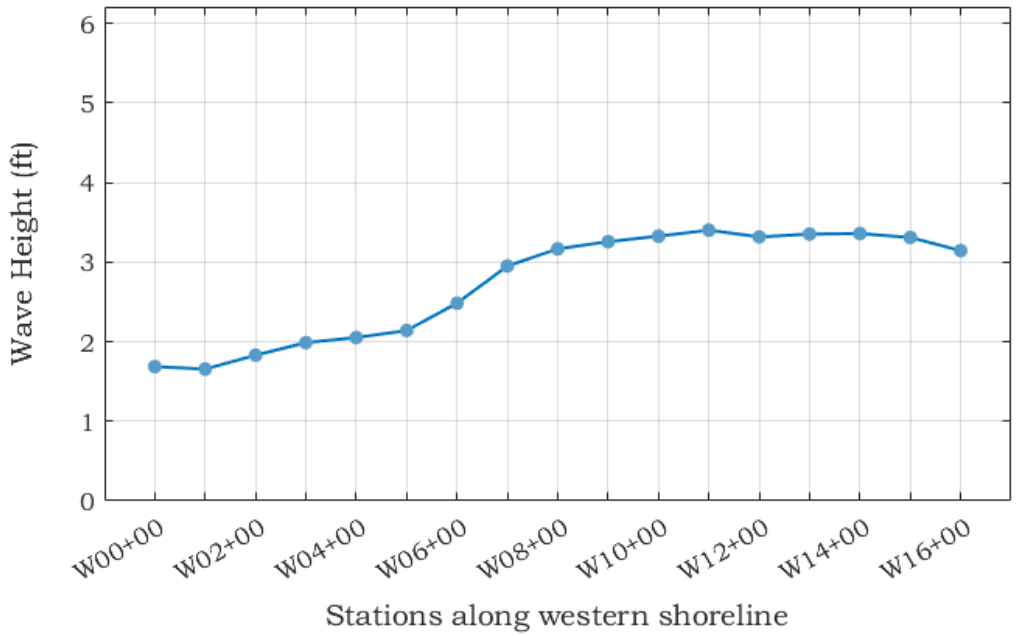

Figure 5.6 Wave model results of the existing conditions along the western shoreline of Eel River Inlet during 100-year storm winds blowing from the Southeast.

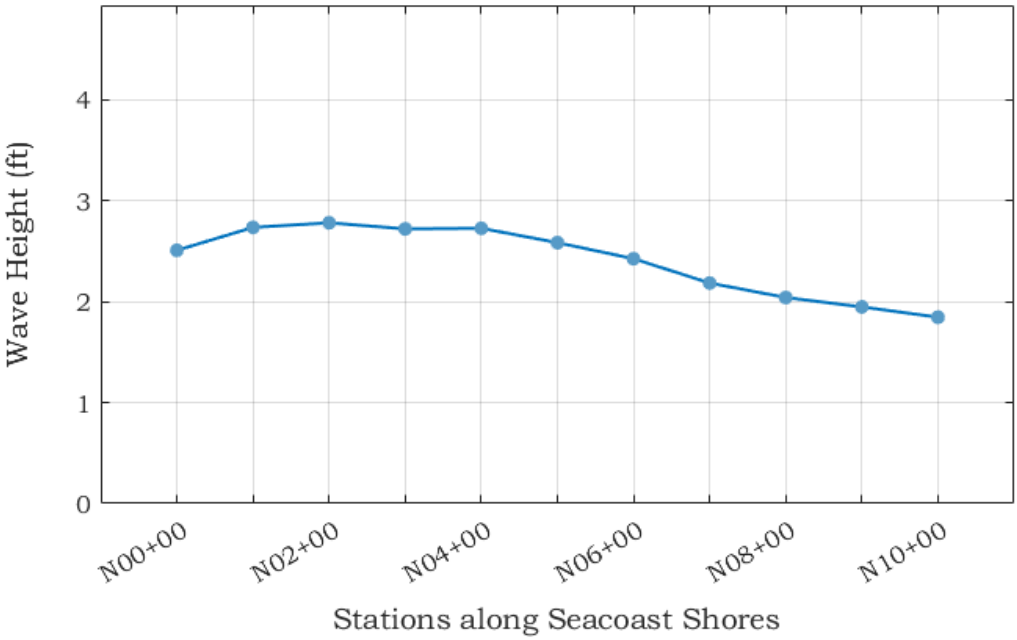

Figure 5.7 Wave model results of the existing conditions along the southern edge of Seacoast Shores during 100-year storm winds blowing from the Southeast.

6 ALTERNATIVES ANALYSIS

Once baseline existing conditions were evaluated and the coastal processes analysis was completed, an alternatives analysis was performed to evaluate potential strategies to mitigate shoreline erosion and enhance navigation safety in Eel River Inlet and the surrounding nearshore areas. The analysis provides site-specific quantitative information for the potential strategies described below to ensure that the most appropriate options are recommended and to support the Town decision-making process. The primary emphasis of the alternative selection process is screening, where the process is to identify the most appropriate alternative(s) based upon a series of criteria. There are no numerical thresholds that identify the best alternative; rather, the screening process is designed to assess a wide range of potential alternatives, and through comparative analysis of various rating criteria, narrow the list of options until only the appropriate remain. While the alternatives are evaluated separately, the recommended solution may include one or more of the appropriate alternatives.

For this analysis, screening criteria focused on the ability of a specific alternative to achieve the project goals: reduction of erosion along the mainland shoreline along the western side of the inlet and ensuring navigation safety. Within the context of meeting project goals, criteria for assessing each alternative included, but were not limited to, design-life, environmental regulatory concerns (i.e. whether an option can be permitted), environmental impacts, and generalized cost (both construction and maintenance).

The project includes three areas of concern (Figure 6.1) that were identified based on their relative impact and/or role in the local coastal processes of the Eel River system. These areas were identified as being dynamic barrier beach areas and/or as areas with unstable shorelines susceptible to erosion that could further expose or threaten existing wetland resource areas and residential property. The primary focus area is along the western shoreline of the inlet, immediately north of the Menauhant Yacht Club. This segment of shoreline is experiencing rapid and ongoing erosion and subsequent loss of the adjacent fringing salt marsh as a direct result of increased tidal currents caused by the evolution of the Washburn Island barrier spit. The western and northern evolution of the spit redirects and constricts tidal flows, thereby increasing the velocity of nearshore currents along the western shoreline of the inlet. Continued elongation and narrowing of the spit also promote further risk of a potential future breach near Washburn Island, where the spit is most susceptible to overwash. In addition, the low-lying nature of the Washburn Island spit indicates that future sea level rise likely will exacerbate breaching of the barrier beach system and increase erosion rates in the future.

Over the next several decades, rapid changes to the barrier beach system and associated inlets/tidal channels likely will create conditions that exacerbate coastal erosion and tidal flooding to areas that may appear well-protected at the present time. At present, overall management of the mainland shoreline is being performed in a reactive manner, based on response to various coastal erosion issues. However, the Town is focused on developing a proactive approach to overall shoreline management, rather than continuing the piece-meal approach to erosion mitigation. With this in mind, the analysis focuses on engineering alternatives that not only address present concerns, but also include potential future issues related to storm overwash and erosion hazards, as well as climate adaptation techniques for the next 20-to-30 years. An assessment of mitigation options ranging from the “do-nothing” alternative to non-structural, structural, and combination structural/non-

structural alternatives was performed utilizing the screening criteria. A comprehensive list includes:

- No action
- Dredge the existing channel (the “status quo”)
- Shortening of the Washburn Island spit
- “Hard” structures
    - Sand trapping structures on the beach (e.g. groins)
    - Shore stabilization structures (e.g. revetments or seawalls)
- “Soft” shore protection measures (e.g. coir logs)
- Combinations of the above options

Figure 6.1 Oblique aerial of Eel River Inlet with specific areas of concern: (1) eroding shoreline and fringe marsh; (2) westerly growth and northerly migration of Washburn Island spit; (3) narrow region of Washburn Island spit susceptible to near future breach.

6.1 Description of Alternatives

As described above, potential mitigation strategies were based on the site-specific nature of the problem (e.g., erosion, tidal currents, local morphology, etc.) in combination with the screening criteria used to determine the most appropriate approach for addressing the ongoing coastal erosion and navigation safety concerns.

6.1.1 No Action Alternative

The no action or do-nothing alternative assumes that the Town will allow natural evolution of the inlet/barrier beach system without mitigation efforts. As a management

tool, it is instructive to evaluate the no action alternative to assess whether proactive management activities are necessary from both a short-term and long-term perspective. Evaluation of coastal processes described in Section 3 and the modeling in Sections 4 and 5, indicate that while Menauhant Yacht Club and other armored properties north of the inlet are relatively stable, continued western growth of the Washburn Island spit across the Eel River entrance will likely accelerate erosion along the western unarmored shoreline of the inlet and threaten private dwellings, as well as cause adverse impacts to wetland resource areas and create additional navigation safety concerns. Based upon the acceleration of erosion rates experienced along the unprotected western bank of the inlet over the last 10-12 years, private infrastructure may be directly impacted within the next 15 years. Alternatively, elongation of the barrier beach will cause additional tidal attenuation, which has been shown to degrade water quality and compromise fisheries and wildlife habitats, unless a new breach forms similar to the conditions experienced prior to Hurricane Bob in 1991. The combination of increased coastal erosion, increased public hazards risks related to navigation safety, and likely degradation in estuarine water quality indicate that the “do-nothing” alternative is not viable.

6.1.2 Dredge Existing Channel

At present, the Town has an active 10-Year Comprehensive Permit that allows dredging as needed within the footprint of the channel outlined by the permit (Figure 6.2; channel dimensions and soundings presented in Appendix A) to maintain navigable waterways. Due to changes in depth and width, the permitted channel consists of three sections: Eel River Entrance Channel, Eel River Channel, and Eel River Extension Channel. The entrance channel has a footprint that is 60 feet wide and a dredge depth of -6 feet relative to MLW. The main channel and extension both have a footprint width of 50 feet, however, their depths are -5 and -4.5 feet MLW, respectively. Dredging of the channel to meet plan specifications listed in the Comprehensive Permit and maintain the “status quo” would require the removal of approximately 8500 cubic yards of material including 85 linear feet of the barrier spit’s distal end.

Results from the hydrodynamic model using adjusted bathymetry to represent this improvement (Figure 6.3) exhibit a reduction in average maximum ebb and flood velocities of 0.80 and 0.76 feet per second (from 4.82 and 4.26 feet per second to 4.02 and 3.50 feet per second), respectively. Although maintaining the “status quo” allows for a reduction in tidal currents and improves navigational safety, this alternative does not provide sufficient redirection of the flow away from the western shoreline of the inlet and may not afford adequate mitigation of future erosion. Additionally, western growth of the spit will continue and frequent (potentially annual) maintenance dredging will be necessary to maintain a navigation channel through the inlet. Since this alternative would not meet the goals of the project by mitigating erosion of the western shoreline and also would require frequent maintenance dredging, this alternative was eliminated from further consideration.

Figure 6.2 Eel River channel location and channel sections as delineated in the 10-Year Comprehensive Permit.

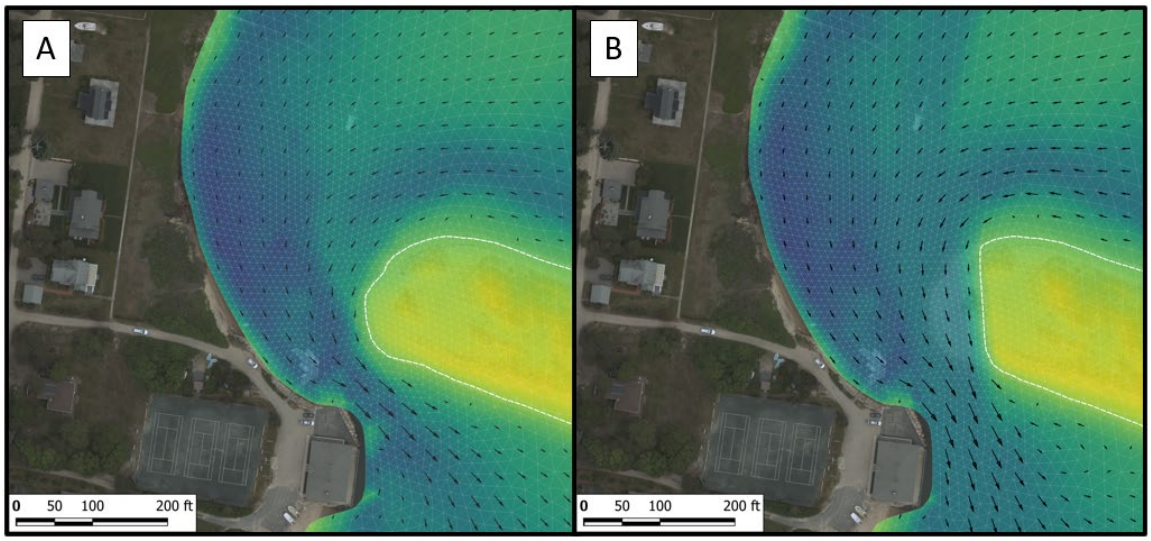

Figure 6.3 Comparison of hydrodynamic model outputs between (A) existing conditions and (B) dredging to meet the channel dimensions and specifications outlined in the 10-Year Comprehensive Permit. Bathymetry is represented by the gradient in color and flow direction and velocities are represented by orientation and size of vector arrows.

6.1.3 Shortening of the Washburn Island Spit

In addition to dredging the channel to the specifications delineated in the 10-Year Comprehensive Permit, dredging the western tip of the Washburn Island spit will create a wider tidal inlet to increase hydraulic efficiency and redirect tidal currents away from the western shoreline of the inlet. In general, the proposed widening of Eel River Inlet extends approximately 350 feet to the historically located terminus of the spit that existed in the early 2000s, as shown in Figure 6.4, and would require the dredging of approximately 31,000 cubic yards of material. Therefore, the shorelines inside the Eel River embayment have experienced both wave and tidal conditions resulting from this alternative at some point in the last few decades; however, a more detailed analysis of potential changes to the local coastal dynamics is warranted.

To simulate the tidal elevations and flow characteristics of the estuary, the same model boundary conditions used to model the existing conditions were used to drive the model with modified “dredged” bathymetry so that a direct comparison of pre- and post-dredge conditions could be made. For the model of proposed post-dredge conditions, the inlet was opened by dredging the spit to a depth of -6 feet MLW within the footprint of the existing channel as specified by the 10-year Comprehensive Permit, and to -3 feet MLW along the remaining cut east of the channel where the spit has been reduced. During periods of peak flow, the greatest reduction in current velocities will occur at the surface of the channel in the narrowest section of inlet, with decreasing influence the greater the distance from the inlet. Figure 6.5 shows an example of the change in velocity between pre- and post-dredge conditions during peak flooding and ebbing tidal flows. Peak flood and ebb velocities, extracted from the center of the channel northeast of Menauhant Yacht Club and averaged across the 29-day temporal domain of the model simulation, were reduced from 4.26 to 1.32 feet per second (reduction of 2.94 feet per second) and from 4.82 to 1.65 feet per second (a reduction of 2.94 and 3.17 feet per second), respectively. It should be noted that a significant increase in velocities is observed in the plots where the spit has been cut as a result in going from a no flow condition to water moving freely across the dredged portion of the spit. Overall, the maximum tidal velocities achieved in the widened inlet channel is over 3 feet per second, which is sufficient to self-scour the inlet channel.

More importantly, the model output exhibits a reduction in the tidal flow velocity along the western shoreline of the inlet, as well as a reduction in nearshore velocities. For flooding cycles of the tide, nearshore velocities are reduced by approximately 1 foot per second along much of the eroding western shoreline of the inlet. A similar reduction can be observed for ebbing flows, however, the area influenced by this change is focused closer to Menauhant Yacht Club. Figure 6.6 shows a contour plot of the change in flow velocity between pre- and post-dredge conditions during maximum ebb velocities as well as a compass plot of instantaneous ebb velocity vectors showing the individual magnitude and orientation of the flow in the center of the channel. The post-dredge conditions exhibit

an improvement in tidal flow angle of greater than 20 degrees towards the north and south directions, or away from the western shoreline, for both flood and ebb tide cycles.

Figure 6.4 Oblique aerial photograph of Eel River Inlet and Washburn Island spit shows the previously existing conditions of the system in December of 2002.

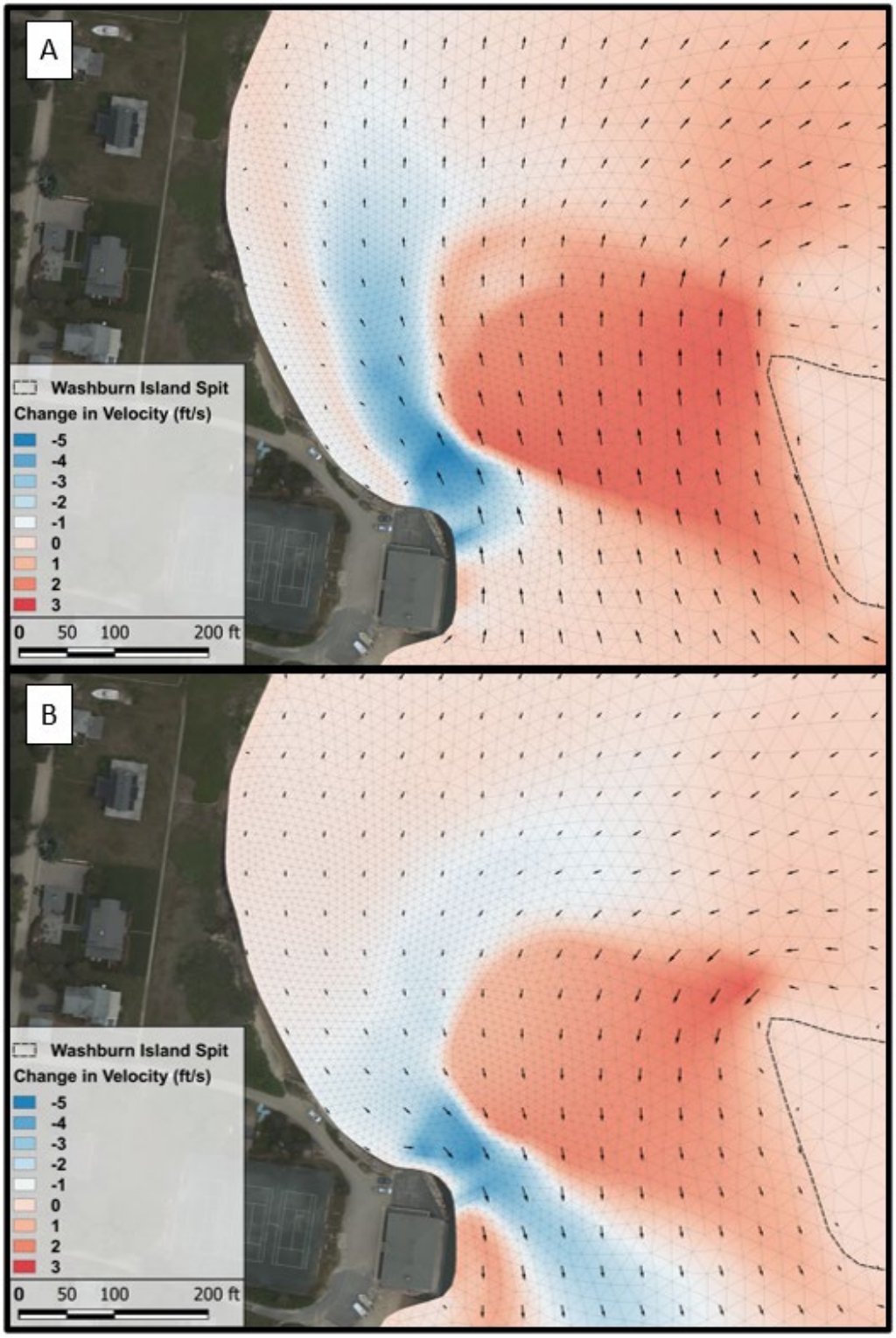

Figure 6.5 Output pre- and post-dredge velocity comparisons from the hydrodynamic model during maximum (A) flooding (B) ebbing tidal flows. Color contours represent change in velocity (where reds indicate an increase in velocity and blues indicate a reduction), while vector arrows represent direction and magnitude of flow of post-dredge condition.

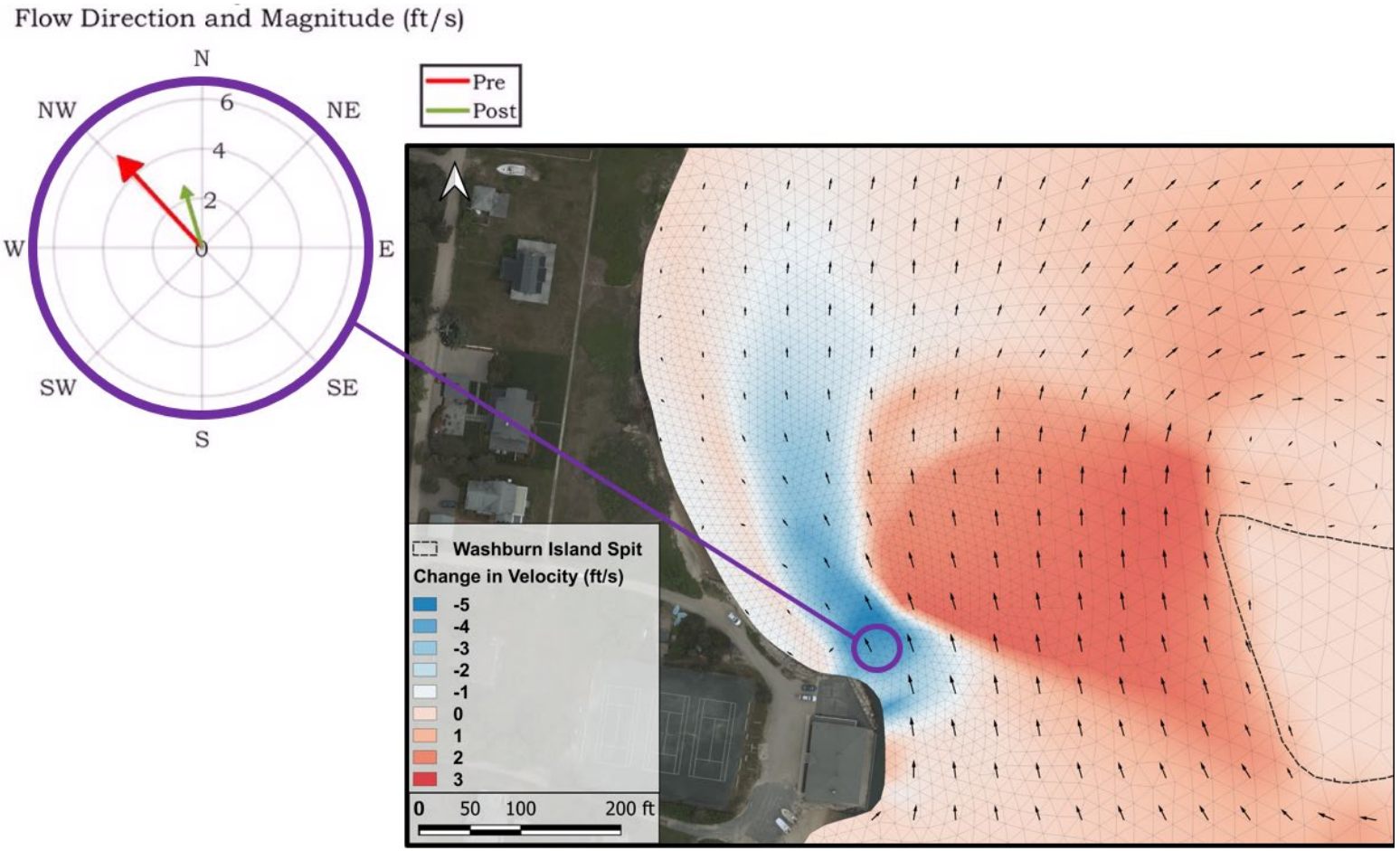

Figure 6.6 Contour plot of change in maximum flooding velocities in the Eel River channel for the post-dredge conditions at Washburn Island. Color contours represent change in velocity where reds indicate an increase in velocity and blues indicate a reduction), while vector arrows magnitude and direction of flow during post-dredge condition. The compass plot in the upper left exhibits pre- (red) and post-dredge (green) velocity magnitudes and direction of flow at a location within the Eel River Entrance Channel.

There is also a potential concern that widening the tidal inlet will allow more wave energy to propagate into the embayment system, causing associated adverse impacts to waterfront property owners north of the yacht club and along the southern point of Seacoast Shores. Using the same post-dredge bathymetry that was used for the hydrodynamic model, the SWAN wave model was rerun for the 100-year southeast storm event (Figure 6.7). Model output of the shows that a portion of the shoreline north of Menauhant Yacht Club will experience higher storm wave energy during the 100-year storm event (Figure 6.8). This area of increased wave energy is generally limited to the region between Thayer Street and Angel Street (approximately between Station 05+00 and Station 11+00 shown on Figure 5.5). Figures 6.9 and 6.10 show each of the modeled wave height observation stations along the western shoreline north of Menauhant Yacht Club and the southern coast of Seacoast Shores for the pre- and

The largest increase in storm wave height is 1.72 feet, observed at Station 06+00 which is the northern most observation location along the focus shoreline along the western bank of the inlet (see Figure 5.5). Therefore, the areas that may experience increased wave heights if the spit is shortened are the same properties that are experiencing rapid erosion from the existing tidal regime. Based on the historical stability of this shoreline when the inlet was wider indicates that the influence of the strong tidal currents on coastal erosion is significantly greater than the influence of increased wave energy from episodic storms.

North of Station 06+00, increases in wave heights become smaller in magnitude and much of shoreline is protected. The shoreline immediately north of the yacht club and south of Thayer Street exhibit an increase in wave heights during a 100-year storm event of 2-5 inches. Figure 6.10 shows the proposed inlet widening would have a negligible effect on wave heights along the southern region of Seacoast Shores. While there is a modest increase in wave heights during a 100-year event, The proposed increase in inlet width and reduction of Washburn Island Barrier spit by 350 feet is not anticipated to have a discernible effect on wave heights on a day-to-day basis.

In general, erosion mitigation and navigational safety are the primary goals, but it also critical to ensure that any potential solution to stabilize the inlet system continues to maintain a healthy littoral system and protect the natural function of the barrier beach. Specifically, potential placement of the dredged material onto the eastern portion of the Washburn Island spit will provide additional width to the barrier beach that may be beneficial coastal wildlife (e.g. nesting shorebird habitat), as well as allowing the beach system to adapt more naturally to relative sea-level rise and the rapidly changing inlet morphology.

Overall, dredging of the existing channel and reduction of approximately 350 feet of the Washburn Island spit affords sustainable and environmentally responsible erosion mitigation of the inlet's shoreline while providing additional protection and improvement to the remaining barrier beach. It is possible that periodic dredging will be required in the long-term to maintain sufficient navigable depths within the channel. Periodic dredging is not a new expense to the Town, as continual dredging to many of the south-facing inlets is needed and is anticipated by the 10-Year Comprehensive Permit. Based on the analysis above, this alternative is likely the most viable option to mitigate shoreline erosion and improve navigation safety within Eel River Inlet and was deemed the preferred alternative.

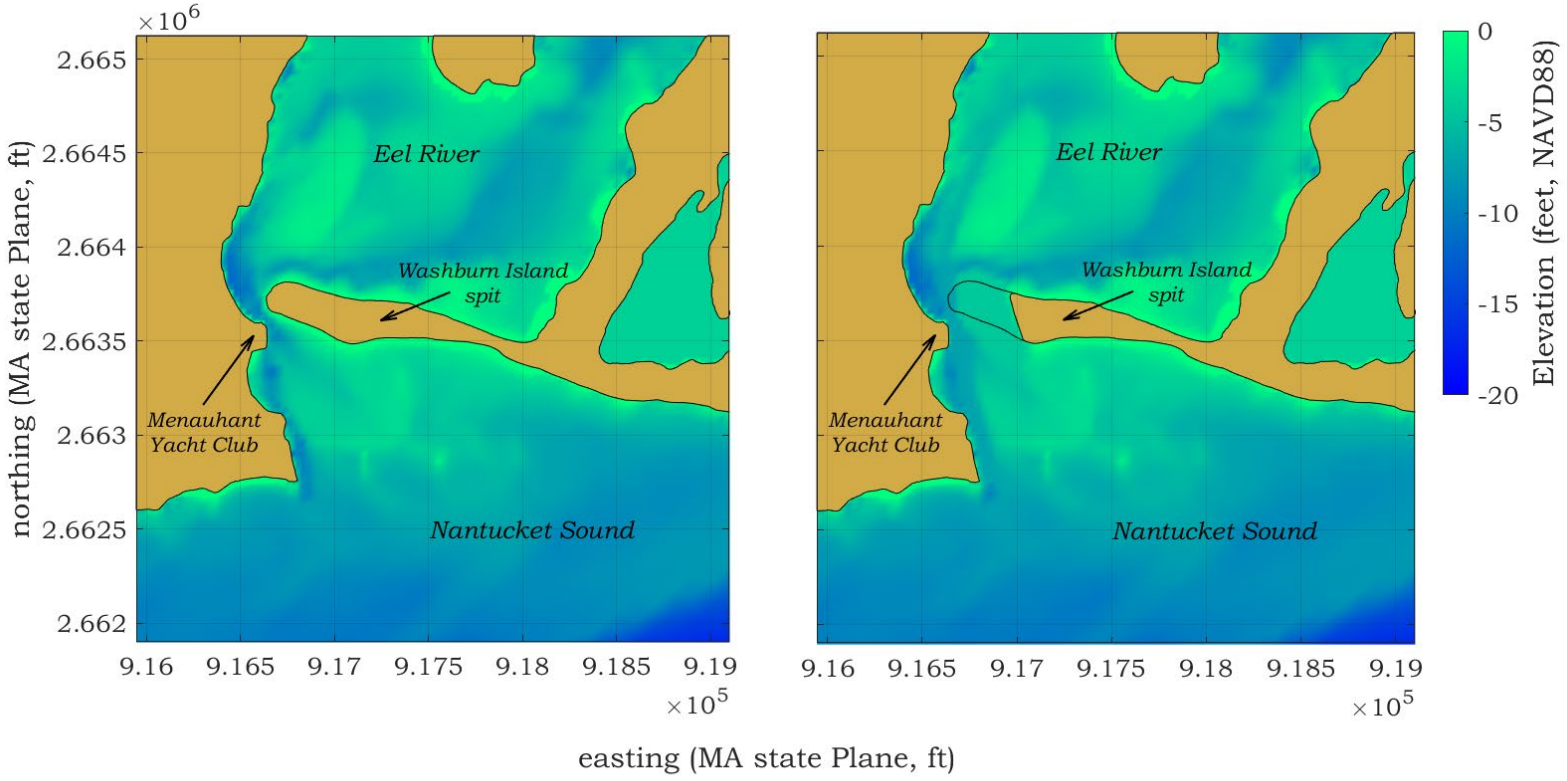

Figure 6.7 Plots of pre- and post-dredge bathymetry in a close-up detail of the Eel River model grid. Post-dredge conditions at Washburn Island include the complete 350-foot proposed cut of the spit. The inlet is dredged to varying depths; -6, -5, and -4.5 ft MLW for the Eel River Entrance Channel, Main Channel, and Extension Channel, respectively; the eastern part of the inlet, in the proposed cut of the spit is dredged to 3 ft MLW.

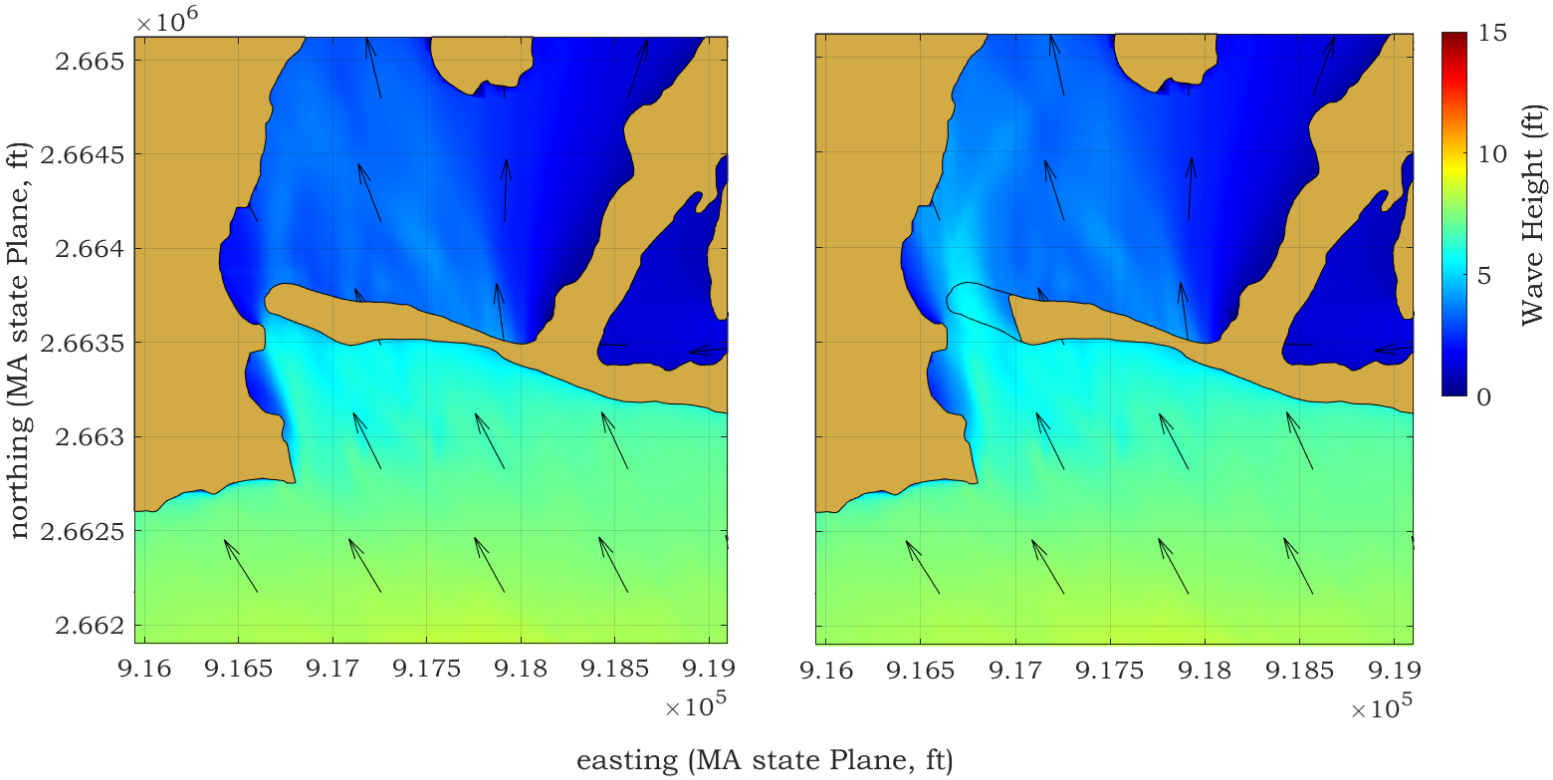

Figure 6.8 Plots of pre- and post-dredge model output significant wave height from the 2D SWAN model for the Eel River nested grid, for 100-year (1%) Southeast wind and offshore wave conditions. Wave heights prescribed at the seaward limit of the grid were on average 8.2 feet, based on outputs from the large-scale regional grid for 100-year (1%) Southeast wind (43.7 kts) and offshore wave conditions (22.4 ft and 11.9 s). Color contours represent significant wave height (H_s), while vector arrows indicate mean wave direction.

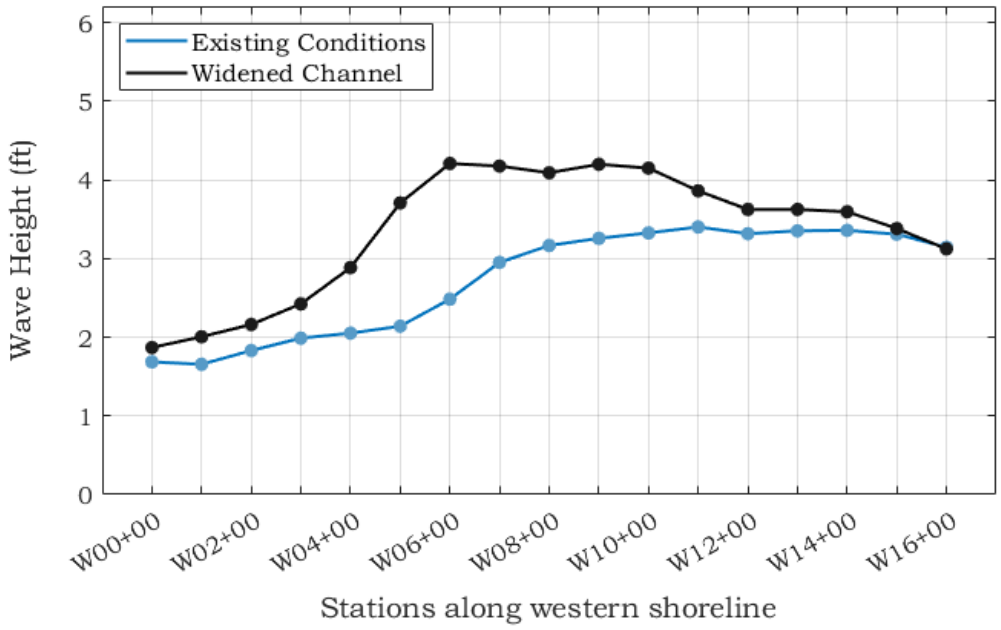

Figure 6.9 Wave model results of the pre- and post-dredge conditions along the western shoreline of Eel River Inlet during 100-year storm winds blowing from the Southeast.

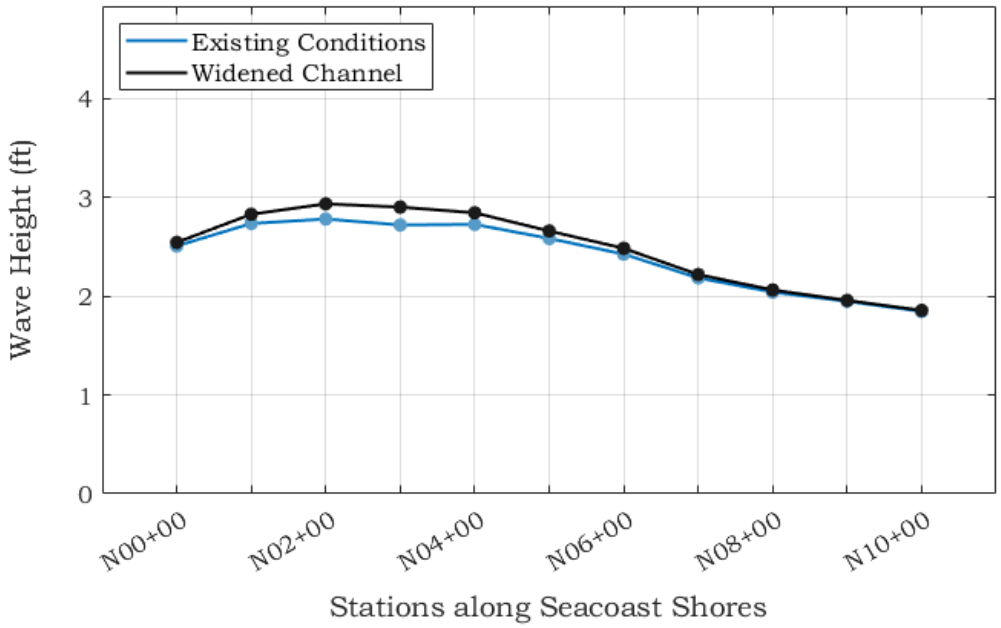

Figure 6.10 Wave model results of the pre- and post-dredge conditions along the southern edge of Seacoast Shores during 100-year storm winds blowing from the Southeast.

6.1.4 "Hard" Structures

The range of "hard" coastal engineering strategies includes methods to directly armor the shoreline (revetments and seawalls), trap sand moving alongshore (groins and jetties), and attenuate wave energy approaching the shoreline (artificial reefs and breakwaters). Overall, these techniques are intended to alter the ability of the natural coastal landforms to respond to coastal erosion processes. Revetments and seawalls directly protect the upland by preventing landward migration of the shoreline. Groins and jetties inhibit, and in some cases prohibit, the alongshore transport of sand. In this capacity, these structures can trap sand

As described previously, numerous coastal engineering structures have been constructed along the south shore of Cape Cod over the past century. The typical purpose for these structures was to stabilize navigation channels or to protect upland infrastructure. A majority of the shore protection structures in this region were constructed during the 30-year period following the 1938 Hurricane. During the two decades that followed, the region was impacted by two more severe hurricanes: the 1944 Hurricane and Hurricane Carol in 1954.

In general, the coastal engineering structures along the Falmouth shoreline performed their intended purpose; however, unanticipated downdrift impacts often occurred to the detriment of both adjacent property owners and environmental resources. The impacts occur as sand is held by the structures thereby starving downdrift areas of sediment. Continued implementation of 'hard' coastal engineering measures will continue this trend of exacerbating downdrift impacts associated with the sediment starved condition of the shoreline.

6.1.4.1 Sand Trapping Structures

The focus shoreline for this project is east-facing adjacent to Eel River Inlet. Due to the orientation of the shoreline and proximity to the inlet, tidal currents alternate flowing along the length of the beach in the north and south directions. As a result, dominant longshore sediment transport varies depending on the direction of the tidal current making sand trapping structures (i.e. groins) a relatively ineffective alternative to mitigate sediment loss and reduce erosion. Additionally, the structures are likely to pose a navigation hazard due to the high velocity currents during peak tidal flows.

It should be noted that general regulatory conditions require that any sand trapping structure remain filled to entrapment throughout the life of the structure. Therefore, costs associated with meeting this requirement need to be included within the total long-term cost associated with any scenarios including groins or breakwaters. In these cases, the nourishment component will be a regulatory requirement, rather than the existing situation where nourishment is placed as funds or opportunities (e.g. navigation dredging) become available. In addition, long-term physical and biological monitoring typically are required as part of any permit; therefore, potential costs associated with these efforts also needs to be considered. This monitoring could include detailed physical monitoring of the beach (i.e. both topographic and bathymetric surveys) and biological sampling of potentially impacted resources (e.g. shellfish and/or horseshoe crabs) periodically over the project design life. This monitoring often is tied to permitting conditions that would require mitigation if results indicate adverse impacts.

Historically, environmental regulatory agencies have discouraged construction of new sand trapping structures along coastal beaches, understanding that there are often adverse impacts to adjacent areas. In some compelling cases, limited use of groins has been permitted, typically to protect at risk critical infrastructure. Even with the direct public safety benefits associated with protection of critical infrastructure projects, the regulatory permitting effort can be extensive (both in time and cost) and mitigation/monitoring efforts are often substantial. It should be noted that these alternatives are generally only considered when it has been demonstrated that no other strategy is available to protect 'at risk' infrastructure without causing greater environmental damage.

Understanding the environmental regulatory hurdles, likely ineffectiveness, and site-specific public safety hazards associated with new groins and/or breakwaters, this alternative is not considered a viable option to mitigate the shoreline erosion occurring in the vicinity of Eel River.

6.1.4.2 Shore Stabilization Structures

The location of Menauhant Yacht Club has remained relatively stable for almost a century, largely due to the stone revetment abutting the inlet which anchors the shoreline in place. Much like sand trapping structures, shore stabilization structures impede natural supply of upland and updrift sediments from maintaining coastal transport processes and may accelerate erosion along downdrift beaches. Ideally, the longevity of shoreline position along the inlet could be enhanced by structural modifications intended to 'optimize' coastal stability without adversely impacting the supply of sediments to downdrift beaches, as much of the material being transported is coming from the south-facing side of Washburn Island due to the east-to-west along this portion of Washburn Island. In general, the alongshore sediment transport direction along the south coast of Falmouth is from west-to-east, driven by the dominant southwest waves; however, a reversal occurs from the Eel River Inlet and along a portion of Washburn Island as a result of the long-term shoreline rotation (see Figure 2.6). This rotation of the shoreline causes refracted waves to actually drive wave-induced transport to the west toward Eel River inlet. Therefore, additional armoring will not reduce sediment transport into the inlet or alleviate the ongoing spit growth at Washburn Island.

Additionally, the steep slope in cross-shore profile (Figure 6.11) indicates that any shoreline stabilization structures along the western bank of the inlet would require extensive engineering to ensure proper scour protection, which could lead to a costly and maintenance intensive design. As initial site observations indicate both Coastal Dune and Salt Marsh resources, it is unlikely that direct armoring of this shoreline could meet the Performance Standards associated with these resource area as required by the Wetlands Protection Act (310CMR 10.00). It is important to note, that while the structure may provide adequate stabilization of the shoreline, it does not mitigate the tidal currents occurring in the inlet. In conjunction with the high cost, potential adverse impacts to coastal resource areas and environmental regulatory concerns associated with implementing engineered 'hard' structures for shore stabilization, there is an added risk of creating a navigation safety hazard. Therefore, shore stabilization structures are not considered a viable alternative to mitigate erosion within Eel River Inlet.

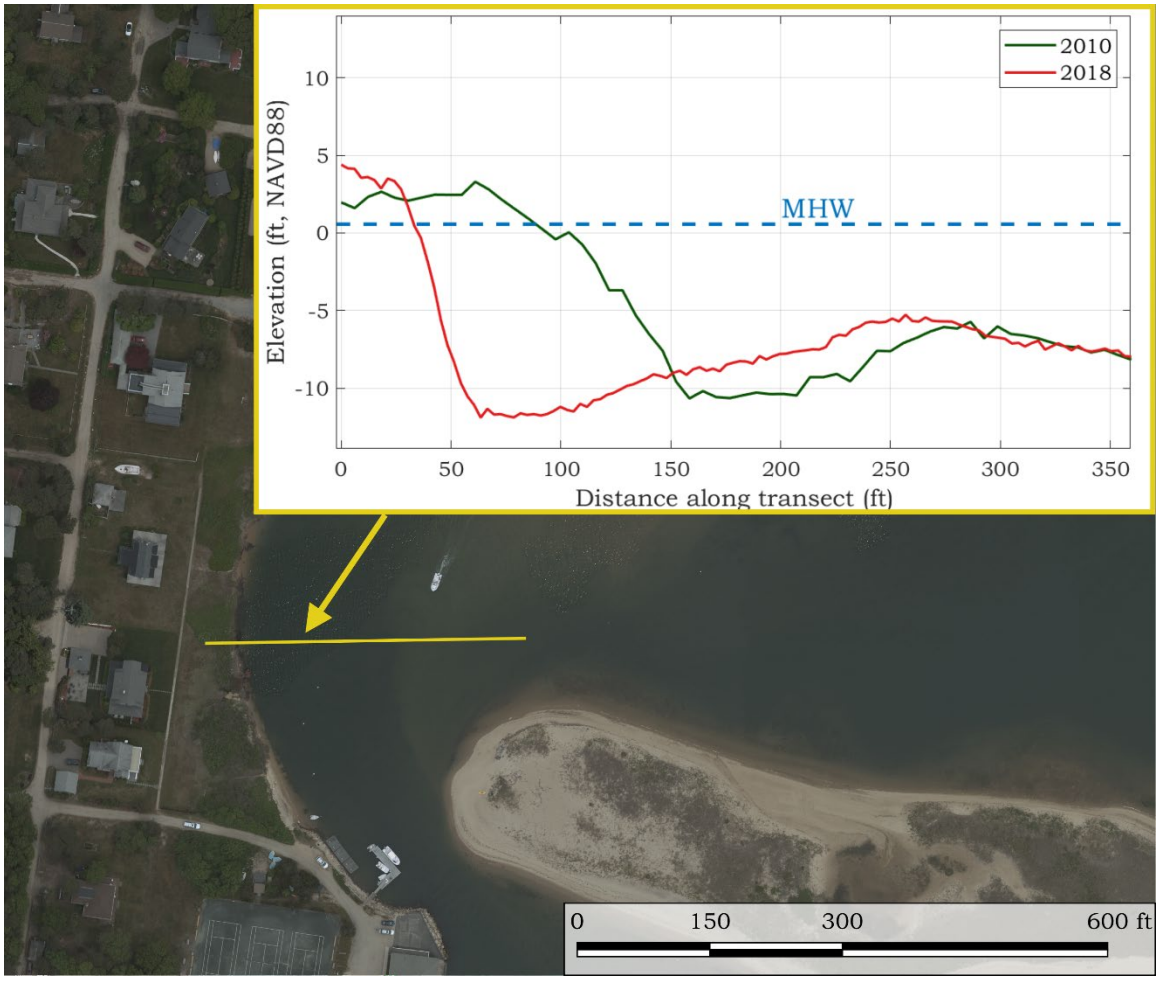

Figure 6.11 Cross-shore profiles for Eel River Inlet from 2010 (green) and 2018 (red).

6.1.5 "Soft" Shore Protection Measures

Over the past few decades, interest in "nature-based" or "soft" engineering approaches for shore protection have become common along shorelines that experience relatively low energy wave conditions. 'Nature-based' coastal erosion mitigation alternatives typically involve a combination of durable natural materials to form rolls or bags that can be anchored along the shoreline to prevent erosion of upland areas, where these measures are often combined with appropriate vegetation for additional stabilization. Other 'soft' shore protection measures can include various forms of dune fencing constructed to trap wind and/or overwash driven sediment. In general, these measures are well-suited for mild wave climates where shoreline erosion is minor. In addition, sites with more energetic wave climates will require frequent maintenance of nature-based erosion control measures. While the south-facing shoreline of Washburn Island has a moderate wave climate, the shorelines within the shelter of the inlet experience more mild wave conditions. However, the "nature-based" approaches are not suitable for the tidally-driven erosional environment associated with the western shoreline at Eel River Inlet, and could only be considered an interim erosion mitigation measure.

Therefore, nature-based approaches do not provide viable alternatives as a stand-alone option for long-term shoreline stabilization.

7 CONCLUSIONS

Based on discussions with the Town, the long-term consideration for stabilization of the shoreline adjacent to the Eel River inlet is 20-to-30 years. Within this time horizon, a range of potential physical processes were considered that might influence the overall longevity of the project. First, regional relative sea-level rise was reviewed, where this "relative" increase in long-term water surface elevations consists of geologic subsidence and the landmass associated with Cape Cod and increases in the regional water level. Historical trends of relative sea-level rise at Woods Hole are well documented by a NOAA tide gauge that has been in operation nearly continuously since 1932. In addition to the historical data, the analysis also includes recent peer reviewed assessments of both projected sea-level increases and projections specifically relating to sea-level rise in the northeastern U.S. determined from a trend analysis of recent data resulting in potential upper bound of sea level rise ranging from 1 to 3 feet. More frequent overwash and breaching of the barrier spit will likely occur, influencing continued northern recession of the barrier system into the Eel River and Waquoit Bay embayment.

The hydrodynamic, wave, and shoreline change analyses of Eel River and Waquoit embayment system provides insight into the dynamics of the existing conditions for this complex tidal estuary. The models developed for this system are valuable tools that greatly expand the utility of data collected from the physical system. The hydrodynamic model was calibrated and validated with previously collected tidal measurements throughout the embayment system. The combined calibration/validation process provides a high level of confidence that the model simulates actual flow characteristics through the channels and waterways. Based on the bathymetry that was used for the hydrodynamic model, a two-dimensional spectral wave model (SWAN) was utilized to extract nearshore wave parameters during extreme storm events, where a lack of *in situ* measurements exists. The natural evolution of the system was measured using a variety of present and historical data sources (such as aerial orthoimagery, LiDAR surveys, and RTK GPS point measurements) that identify shoreline positions. The shoreline change analysis was used in conjunction with the hydrodynamic and wave models to assess a range of potential erosion mitigation options.

The results of the hydrodynamic and shoreline change analysis illustrate the mechanisms likely responsible for the observed erosion along the western shoreline of the inlet. Western growth of the Washburn Island barrier spit reduces the width of the inlet and shifts the channel closer to the western shoreline of the inlet. The narrowing inlet constricts tidal flow between the embayment and Nantucket Sound resulting in higher velocity currents that continue to scour the shoreline as the channel migrates west in response to the elongating spit. Thus, any efforts to mitigate erosion without alteration to the existing hydrodynamics of the system will likely prove ineffective.

The evaluation of potential mitigation strategies shows that some type alternative of dredging is likely the best course of action to improve the hydrodynamics of the inlet. An analysis of two dredging alternatives (dredging as originally permitted and widening the inlet by shortening the spit to previously existing conditions) was conducted to review the potential impacts and improvements that would result from each alternative. The

results show that maintaining the existing permitted channel will create little to no remediation of ongoing erosion and would require more frequent maintenance dredging. Widening the inlet and shortening the spit by approximately 350 feet will reduce flow velocities as well as redirect currents away from the eroding shoreline, with the additional benefit of improving navigation safety. Therefore, shortening the Washburn Island spit was determined to be the preferred alternative for achieving the long-term project goals. To further pursue this alternative, it would be worthwhile for the Town to set up a MEPA pre-application meeting to present the analysis and discuss additional analyses that may be required to support advancing the project.

REFERENCES

Booij, N., Ris, R.C., & Holthuijsen, L. H. (1999). A third-generation wave model for coastal regions: 1. Model description and validation. Journal of geophysical research: Oceans, 104(C4), 7649-7666.

DeConto, R., & Pollard, D. (2016). Contribution of Antarctica to past and future sea-level rise. Nature, 531(7596), 591–597.

DeConto, R. & Kopp, R. (2017). Massachusetts Sea Level Assessment and Projections. Technical memorandum.

Federal Emergency Management Agency, Flood Insurance Study, Barnstable County, Massachusetts (All Jurisdictions), Effective July 6, 2021

Howes, B., Samimy, R., Schlezinger, D., Eichner, E., Kelley, S., Ramsey, J., & Detjens, P. (2013). Linked watershed− embayment approach to determine critical nitrogen loading thresholds for the Waquoit Bay and Eel Pond embayment system, towns of Falmouth and Mashpee, Massachusetts. Massachusetts Department of Environmental Protection, Boston, MA. *Massachusetts Estuaries Proj. Final Rep (205 p)*.

IPCC, 2013: Climate Change 2013: Contribution of Working Group I to the Fifth Assessment Report of the Intergovernmental Panel on Climate Change. Cambridge University Press, Cambridge, United Kingdom and New York, NY, USA.

Kopp, R., Horton, R., Little, C., Mitrovica, J., Oppenheimer, M., Rasmussen, D. J., & Tebaldi, C. (2014). Probabilistic 21st and 22nd century sea-level projections at a global network of tide-gauge sites. *Earth's future*, *2*(8), 383-406.

Kopp, R., DeConto, R., Bader, D., Hay, C., Horton, R., Kulp, S., Oppenheimer, M., Pollard, D., & Strauss, B. (2017). Evolving Understanding of Antarctic Ice-Sheet Physics and Ambiguity in Probabilistic Sea-Level Projections, Earth's Future, 5.

Rignot, E., Velicogna I., van den Broeke M., Monaghan A., & Lenaerts J. T. M. (2011), Acceleration of the contribution of the Greenland and Antarctic ice sheets to sea level rise, Geophysical Research Letter, 38.

Van Vuuren, D., Edmonds, J., Kainuma, M., Riahi, K., Thomson, A., Hibbard, K., & Lamarque, J.-F. (2011), The representative concentration pathways: an overview. Climatic Change, 109, 5-31.

APPENDIX A

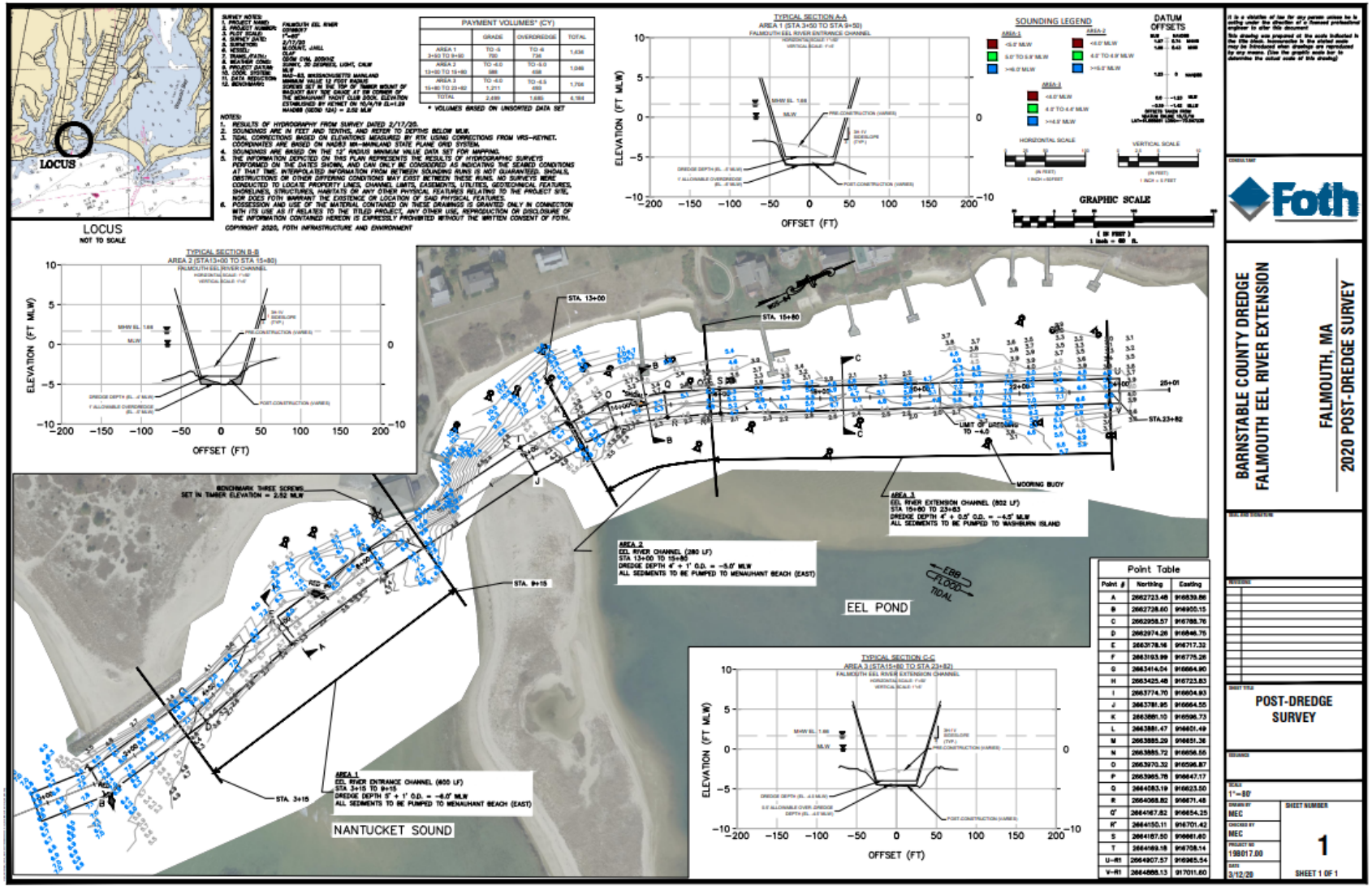

Figure A. 1 Post dredge survey conducted February 17, 2020, included with channel location dimensions as determined by the 10-Year Comprehensive Permit.